SPRINGER BRIEFS IN ENERGY
COMPUTATIONAL MODELING OF ENERGY SYSTEMS

Haibing Shao · Philipp Hein
Agnes Sachse · Olaf Kolditz

Geoenergy Modeling II

Shallow Geothermal Systems

Springer

SpringerBriefs in Energy

Computational Modeling of Energy Systems

More information about this series at http://www.springer.com/series/8903

Haibing Shao • Philipp Hein • Agnes Sachse
Olaf Kolditz

Geoenergy Modeling II

Shallow Geothermal Systems

Springer

Haibing Shao
Department of Environmental Informatics
Helmholtz Centre for Environmental Research
Leipzig, Germany

Agnes Sachse
Department of Environmental Informatics
Helmholtz Centre of Environmental Research-UFZ
Leipzig, Germany

Philipp Hein
Helmholtz Centre of Environmental Research UFZ
Department of Environmental Informatics
University of Applied Science Leipzig HTWK
Faculty of Mechanical and Energy Engineering
Leipzig, Germany

Olaf Kolditz
Environmental Informatics
Helmholtz-Zentrum für Umweltforschu
Environmental Informatics
Leipzig, Sachsen, Germany

ISSN 2191-5520 ISSN 2191-5539 (electronic)
SpringerBriefs in Energy
ISBN 978-3-319-45055-1 ISBN 978-3-319-45057-5 (eBook)
DOI 10.1007/978-3-319-45057-5

Library of Congress Control Number: 2016935862

Printed on acid-free paper

This Springer imprint is published by Springer Nature
The registered company is Springer International Publishing AG
The registered company address is Gewerbestrasse 11, 6330 Cham, Switzerland

Foreword

This tutorial presents the introduction of the open-source software *OpenGeoSys* (OGS) for shallow geothermal applications. This tutorial is the result of a close cooperation within the OGS community (www.opengeosys.org). These voluntary contributions are highly acknowledged.

The book contains general information regarding the numerical simulation of heat transport process in the shallow subsurface, which is closely coupled with the operation of borehole heat exchangers (BHE) and ground source heat pumps (GSHP). In addition to the introduction of how to establish such a model, benchmark examples and a real-world test case is presented in this book, which leads to concrete advices for the end users when exploring shallow geothermal energy.

This book is intended primarily for graduate students and applied scientists who deal with geothermal system analysis. It is also a valuable source of information for professional geoscientists wishing to advance their knowledge in numerical modeling of geothermal processes, including convection and conduction. As such, this book will be a valuable help in geothermal modeling training courses.

There are various commercial software tools available to solve complex scientific questions in geothermics. This book will introduce the user to an open-source numerical software code for geothermal modeling which can even be adapted and extended based on the needs of the researcher.

This tutorial is part of a series that will represent further applications of computational modeling in energy sciences. Within this series, the planned tutorials related to the specific simulation platform OGS. The planned tutorials are:

- OpenGeoSys Tutorial. Basics of Heat Transport Processes in Geothermal Systems, Böttcher et al. (2015)
- OpenGeoSys Tutorial. Shallow Geothermal Systems, Shao et al. (2016), this volume
- OpenGeoSys Tutorial. Enhanced Geothermal Systems, Watanabe et al. (2016*)
- OpenGeoSys Tutorial. Geotechnical Storage of Energy Carriers, Böttcher et al. (2016*)

- OpenGeoSys Tutorial. Models of Thermochemical Heat Storage, Nagel et al. (2017*)

These contributions are related to a similar publication series in the field of environmental sciences, namely:

- Computational Hydrology I: Groundwater flow modeling, Sachse et al. (2015), DOI 10.1007/978-3-319-13335-5, http://www.springer.com/de/book/9783319133348
- OpenGeoSys Tutorial. Computational Hydrology II: Density-dependent flow and transport processes, Walther et al. (2016*)
- OGS Data Explorer, Rink et al. (2016*)
- Reactive Transport Modeling I (2017*)
- Multiphase Flow (2017*)

(*publication time is approximated).

Leipzig, Germany
June 2016

Haibing Shao
Philipp Hein
Agnes Sachse
Olaf Kolditz

Acknowledgments

We deeply acknowledge the continuous scientific and financial support to the *OpenGeoSys* development activities by the following institutions:

We would like to express our sincere thanks to HIGRADE in providing funding for the *OpenGeoSys* training course at the Helmholtz Centre for Environmental Research.

We also wish to thank the *OpenGeoSys* developer group (ogs-devs@googlegroups.com) and the users (ogs-users@googlegroups.com) for their technical support.

Contents

List of Contributors

Philipp Hein, Faculty of Mechanical and Energy Engineering, University of Applied Science Leipzig – HTWK, Leipzig, Germany

Department of Environmental Informatics, Helmholtz Centre of Environmental Research – UFZ, Leipzig, Germany

Olaf Kolditz, Department of Environmental Informatics, Helmholtz Centre of Environmental Research – UFZ, Leipzig, Germany

Applied Environmental System Analysis, Technical University of Dresden, Dresden, Germany

Agnes Sachse, Department of Environmental Informatics, Helmholtz Centre of Environmental Research – UFZ, Leipzig, Germany

Haibing Shao, Department of Environmental Informatics, Helmholtz Centre of Environmental Research – UFZ, Leipzig, Germany

Faculty of Geoscience, Geotechnics and Mining, Freiberg University of Mining and Technology – TUBAF, Freiberg, Germany

Chapter 1
Introduction

1.1 Geothermal Systems

> Geothermal energy is a promising alternative energy source as it is suited for base-load energy supply, can replace fossil fuel power generation, can be combined with other renewable energy sources such as solar thermal energy, and can stimulate the regional economy.

The above text is quoted from an editorial of a new open-access journal Geothermal Energy (Kolditz et al. 2013), which advocates the potential of this renewable energy resource for both heat supply and electricity production. Indeed, *Geothermal energy* has recently became an essential part in many research programmes worldwide. The current status of research on geoenergy (including both geological energy resources and concepts for energy waste deposition) in Germany and other countries has been compiled in a thematic issue on "Geoenergy: new concepts for utilization of geo-reservoirs as potential energy sources" (Scheck-Wenderoth et al. 2013). The Helmholtz Association dedicated a topic on geothermal energy systems into its next 5-year-program from 2015 to 2019 (Huenges et al. 2013).

When looking at different types of geothermal systems, it can be distinguished between shallow, medium, and deep systems in general (cf. Fig. 1.1). Installations of shallow systems are allowed down to 100–150 m of subsurface, which includes soil and shallow aquifers. If going further down, the medium systems are associated with hydrothermal resources and may be suited for underground thermal storage (Bauer et al. 2013). Deep systems are connected to petrothermal sources and need to be stimulated, in order to increase the hydraulic conductivity for heat extraction by fluid circulation (Enhanced Geothermal Systems—EGS).

H. Shao et al., *Geoenergy Modeling II*, SpringerBriefs in Energy,
DOI 10.1007/978-3-319-45057-5_1

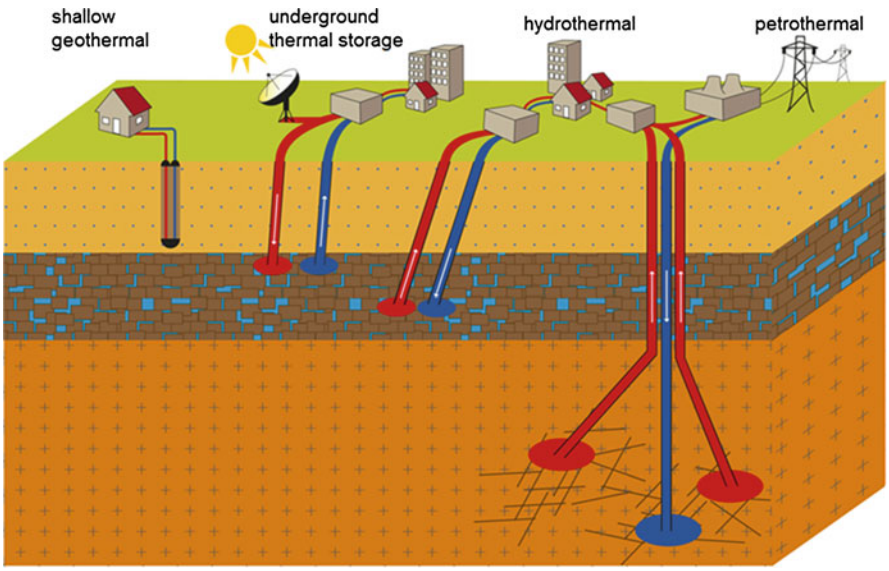

Fig. 1.1 Overview of different types of geothermal systems: shallow, medium and deep systems (Huenges et al. 2013)

1.2 Geothermal Resources

In general, the corresponding temperature regimes at different depths depend on the geothermal gradient (Clauser 1999). Some areas benefit from favourable geothermal conditions with amplified heat fluxes, e.g., in the North German Basin, Upper Rhine Valley, and the Molasse Basin of Germany (Cacace et al. 2013). Conventional geothermal systems mainly rely on heated water (hydrothermal systems) that approaches the near-surface. Therefore they are regionally limited to near continental plate boundaries and volcanoes. Nevertheless, this book will focus on the numerical modelling of extracting shallow geothermal resources. In particular, this book will explain in details how to numerically simulate the evolving soil temperature in response to heat extraction from borehole heat exchangers.

Before diving down into the numerical world, let's have an overview on how much energy is stored in the subsurface that we are standing on. First, here are some interesting numbers about the solid earth:

- The mean surface temperature is abut 15 °C.
- Despite of strong fluctuations of the surface temperature, the soil or rock temperature beneath 15–20 m of depth is largely constant.
- The geothermal gradient in the upper part is about 30 K per kilometer depth ($0.03\,\mathrm{Km}^{-1}$). In another word, from the surface downwards, the average soil temperature will increase 3° by every 100 m.

So how much energy can we extract from the shallow subsurface?

When looking into the shallow geothermal systems, it is rather unlikely to have a 20–30 K temperature drop as in the deep geothermal reservoirs. However, if the temperature of the shallow subsurface is decreased by only 0.5–2 °C, it will still generate large amount of energy. For example, Zhu et al. (2010) evaluated the geothermal potential of the city Cologne, and they found that a temperature decrease of 2 °C in the 20 m thick aquifer will yield enough energy that is more than the city's annual space heating demand. Using a similar approach, Arola and Korkka-Niemi (2014) assessed the effect of urban heat islands on the geothermal potential in three cities in southern Finland. It turns out that, because of the urban heat island effect, 50–60 % more heat can be supplied from shallow subsurface in the urban area, in comparison to rural areas.

1.3 Utilizing Shallow Geothermal Resources

Now the energy embedded in the shallow subsurface is more than plenty. How can it be utilized? Currently, the most widely applied technology is the so-called Ground Source Heat Pump (GSHP) system. Such system is typically composed of three inter-connected parts (cf. Fig. 1.2), namely (1) the ground loop, (2) the heat pump, and (3) the in-door loop.

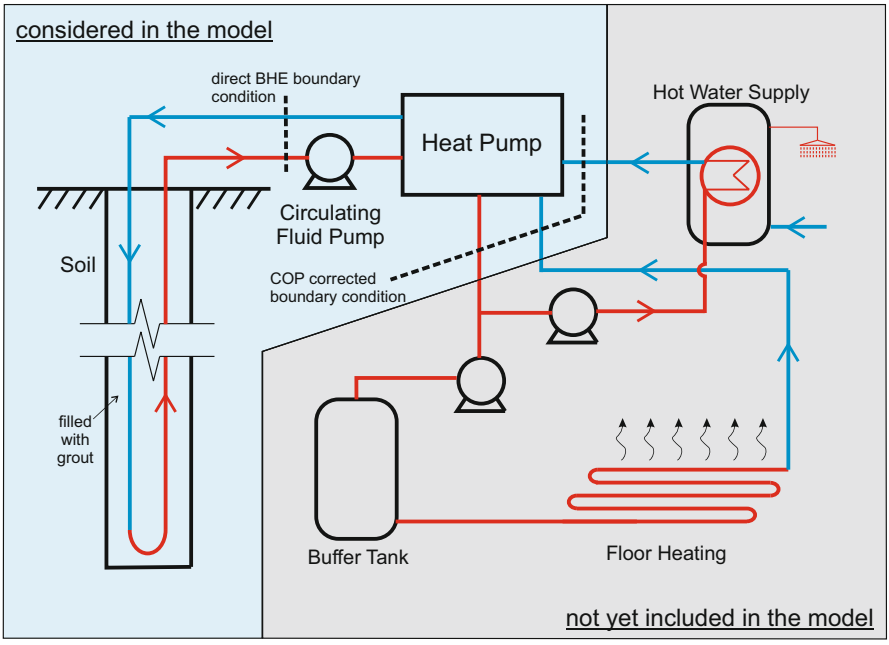

Fig. 1.2 Overview of the Ground Source Heat Pump (GSHP) system, reproduced after Zheng et al. (2016)

- The ground loop is composed of one or multiple borehole heat exchangers (BHE). Their main function is to extract heat from the shallow subsurface for building heating, or injecting heat while providing cooling. This is typically achieved by installing closed loop tubes, buried vertically or horizontally in the ground, and circulating refrigerant through the pipes.
- The function of the heat pump, is to elevate the low-grade heat from the ground loop, to high-grade heat that can directly be applied for room heating or hot water supply.
- As for the in-door loop, it is designed to transport and dissipate high-grade heat or code through the building.

In this book, the numerical modelling software OpenGeoSys (OGS) will be employed to model the borehole heat exchanger and heat pump part, more specifically to simulate the dynamics behaviour of soil temperature due to GSHP operation (Fig. 1.3).

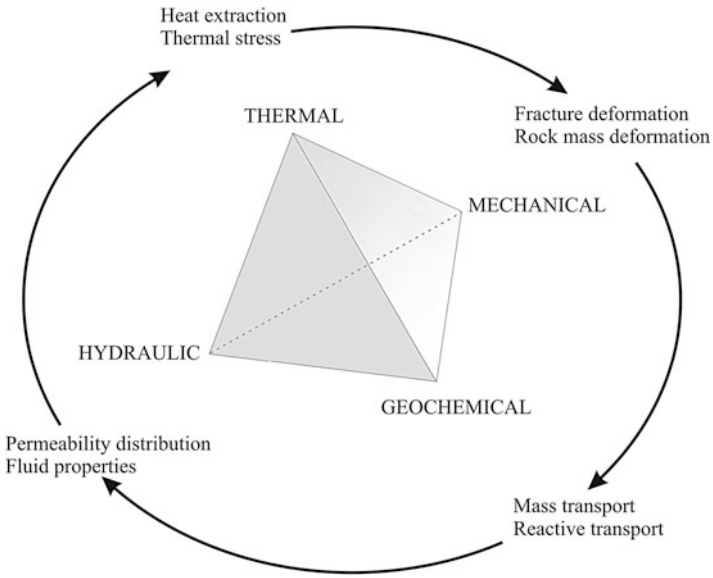

Fig. 1.3 THMC coupling concept. OGS is a scientific open-source initiative for numerical simulation of thermo-hydro-mechanical/chemical (THMC) processes in porous and fractured media, continuously developed since the mid-eighties. The OGS code is targeting primarily applications in environmental geoscience, e.g. in the fields of contaminant hydrology, water resources management, waste deposits, or geothermal systems, but it has also been applied to new topics in energy storage recently

1.4 Tutorial and Course Structure

This tutorial "Computational Energy Systems II: Shallow Geothermal System" contains several parts. In Chap. 2, the governing equations of the numerical model will be defined. Chapter 3 shows the user how to set up a project to simulate heat transport processes induced by a BHE operation. To construct the mesh used in Chap. 3, a meshing tool will be needed, which is introduced in Chap. 4. The developed OGS model will be verified in Chap. 5, with three different benchmarks. A realistic application is presented in Chap. 6, and the knowledge from the modelling study will be further discussed. This tutorial can also be used in combination with the following material

- OGS training course on geoenergy aspects held by Norihiro Watanabe in November 2013 in Guangzhou,
- OGS training course on CO_2-reduction modelling held by Norbert Böttcher in 2012 in Daejon, South Korea,
- OGS benchmarking chapter on heat transport processes by Norbert Böttcher,
- University lecture material (TU Dresden) and presentations by Olaf Kolditz.

By visiting the OGS webpage at https://docs.opengeosys.org/books/shallow-geothermal-systems, interested readers can obtain the dataset used in this book, to conduct their own simulations for the ground source heat pump system.

Chapter 2
Theory: Governing Equations and Model Implementations

Here in this chapter of the tutorial, the governing equations of heat transport processes inside and around the Borehole Heat Exchangers (BHEs) will be presented. Also, discussions will focus on the numerical techniques applied in OpenGeoSys to solve it. Note that the method implemented here is not the creative work of the authors, but rather a collection of contributions from the scientific community. The formulation of heat exchange between BHEs and the surrounding soil, was proposed by Al-Khoury et al. (2010). This formulation was later-on adopted by Diersch et al. (2011a,b) into the commercial software FEFLOW. In this work, the same idea of Al-Khoury and Diersch was implemented into the open-source scientific software OpenGeoSys, to simulate the heat transport process in response to BHEs. For interested readers, the FEFLOW book (Diersch 2014) also provides a good reference for the better understanding of the Finite Element Method (FEM).

2.1 Conceptual Model of the BHEs

To exchange heat with the surrounding soil and rock, borehole heat exchangers are installed in the subsurface. They have different designs and configurations. The most commonly applied BHEs are four different types, including the single U-tube (1U), double U-tube (2U), coaxial centred (CXC) and coaxial annular (CXA) types. The U-type BHEs are named after the U shaped pipelines laid vertically along the borehole. The number 1 or 2 refer to how many pairs of U tubes are in the same borehole. To illustrate this, Fig. 2.1 shows the horizontal cross-section of a 1U type BHE. Notice that the U tubes are normally sealed by grout materials, and not in direct contact with the soil. For a typical BHE, a refrigerant fluid is circulating inside of the U tube, absorbing or releasing heat from or into the surrounding grout and soil.

H. Shao et al., *Geoenergy Modeling II*, SpringerBriefs in Energy,
DOI 10.1007/978-3-319-45057-5_2

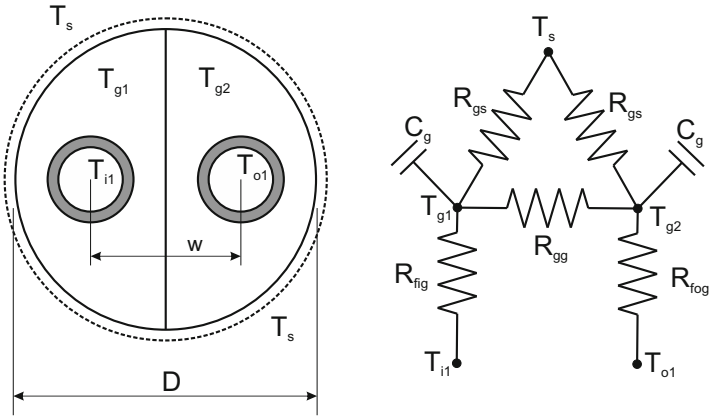

Fig. 2.1 Configuration of the 1U type BHE and its corresponding resister-capacitor concept, reproduced after the FEFLOW book Diersch (2014)

In order to numerically simulate the heat transfer process inside a BHE, the device is further conceptualized by the so-called Resister-Capacitor model. This idea originates from the discipline of electrical engineering. In a electrical circuit, if the electric current is hindered by a component, it is called a Resistor. When a component is capable of storing the electricity, then it is named as a Capacitor. So the same concept can also be applied to the heat transport in a BHE. Taking the 1U type of BHE in Fig. 2.1 as an example, four temperature values are assigned to different compartments. They are T_s, T_{i1}, T_{o1}, T_{g1} and T_{g2}, referring to the temperatures of the surrounding soil, the inlet pipe, the outlet pie, the fisrt (left) and the second (right) grout zone respectively. As a convention, it is always assumed that the first grout zone is the one surrounding the inlet pipe. Following this concept, the heat transfer between the pipe and the soil can be divided into five pathways: (1) between inlet pipe and first grout zone; (2) between outlet pipe and second grout zone; (3) between the two grout zones; (4) between first grout zone and the soil; (5) between second grout zone and the soil. The heat flux q_n on each of these pathways, are driven by the temperature difference and regulated by the heat transfer coefficient Φ. For example, the heat flux from inlet pipe to the first grout zone can be calculated by

$$q_n = \Phi_{fig} \left(T_{i1} - T_{g1} \right), \tag{2.1}$$

in which the heat transfer coefficient Φ is inversely dependent on the product of heat resistance R and specific exchange area S

$$\Phi = \frac{1}{RS} \tag{2.2}$$

Depending on the pathway, there will be different heat transfer coefficients, denoted as Φ_{fig}, Φ_{fog}, Φ_{gg} and Φ_{gs}. Details regarding how to calculate these heat transfer coefficients can be found in Diersch et al. (2011a).

2.2 Governing Equations

2.2.1 Governing Equations for the Heat Transport Process in Soil

For the heat transport process in the soil, the development of soil temperature T_s is contributed by both the heat convection of the fluid f in the soil and the heat conduction through the soil matrix. Let ρ^s, ρ^f and c^s, c^f be the density and specific heat capacity of fluid f and soil s. If assuming the soil matrix is fully saturated with groundwater, the Darcy velocity of which is described by the vector $\mathbf{v}$, then the conservation equation writes as

$$\frac{\partial}{\partial t}\left[\epsilon\rho^f c^f + (1-\epsilon)\rho^s c^s\right] T_s + \nabla\cdot\left(\rho^f c^f \mathbf{v} T_s\right) - \nabla\cdot(\Lambda^s\cdot\nabla T_s) = H_s, \tag{2.3}$$

with Λ^s the tensor of thermal hydrodynamic dispersion and H_s the source and sink terms for heat. When considering the heat exchange between the BHEs and the soil, the above governing equation is subject to a Cauchy-type of boundary condition:

$$-(\Lambda^s\cdot\nabla T_s) = q_{nT_s}. \tag{2.4}$$

2.2.2 Governing Equations for the Borehole Heat Exchangers

The governing equations for the BHE write differently, depending on whether it is for the pipelines or for the grout zones. Let Ω_k refer to the different compartments in the BHE. For the pipelines ($k = i1, o1$), the heat transport process is dominated by the convection of the refrigerant r with a flow rate $\mathbf{u}$.

$$\begin{aligned}
&\rho^r c^r \frac{\partial T_k}{\partial t} + \rho^r c^r \mathbf{u}\cdot\nabla T_k - \nabla\cdot(\Lambda^r\cdot\nabla T_k) = H_k \text{ in } \Omega_k \\
&\text{with Cauchy type of BC}: \quad -(\Lambda^r\cdot\nabla T_k)\cdot n = q_{nT_k} \text{ on } \Gamma_k \\
&\qquad\qquad\qquad\qquad\qquad\qquad \text{for } k = i1, o1, (i2, o2)
\end{aligned} \tag{2.5}$$

Λ^r stands for the hydrodynamic thermo-dispersion of the refrigerant,

$$\Lambda^r = (\lambda^r + \rho^r c^r \beta_L \|\boldsymbol{u}\|)\,\delta. \tag{2.6}$$

For the grout zones ($k = g_1, g_2 \ldots$), the heat transport is mainly controlled by the heat dissipation.

$$(1-\epsilon^g)\rho^g c^g \frac{\partial T_k}{\partial t} - \nabla \cdot [(1-\epsilon^g)\lambda^g \cdot \nabla T_k] = H_k \text{ in } \Omega_k$$
$$\text{with Cauchy type of BC}: \quad -[(1-\epsilon^g)\lambda^g \cdot \nabla T_k] \cdot n = q_{nT_k} \text{ on } \Gamma_k$$
$$\text{for } k = g1, (g2, (g3, g4)). \quad (2.7)$$

2.2.3 Calculation of the Cauchy Type of Boundary Conditions

The Cauchy type of boundary conditions exit for the soil part, for the pipelines, and also for the grout zones. They are regulated by the heat exchange terms between these compartments. In general, the heat exchange flux q_{nT_k} is proportional to the temperature difference in the neighbouring compartments [see Eq. (2.1)]. The calculation of these flux terms is summarized in Table 2.1.

2.3 Numerical Model

2.3.1 Mesh Arrangement

To simulate the heat transport process together with BHEs, a dual-continuum approach has been adopted to treat the soil and BHEs parts separately. For the soil part, prism elements are used to discretize the 3D domain. In addition to that, 1D line elements along the edge of the prism elements are chosen to form the second domain, which represents the BHE. The example illustrated in Fig. 2.2 contains a mesh structure with 12 nodes and six element. Node "0"–"11" forms the three prism elements, which refers to the soil domain. The BHE domain is composed of three line elements in red color. Notice the node "2", "5", "8" and "11" are both employed by the prim and line elements. As a result, the total number of nodes remains the same and the number of elements slightly increases. In the soil domain, there is only one primary variable on each node, which is the soil temperature. While in the BHE domain, each node has 4, 8, or 3 primary variables, depending on the type of the BHE. Table 2.2 summarizes the combination of primary variables for different BHE types.

The text box below shows the content of a mesh file, configured according to the geometry in Fig. 2.2. Under the key word `$NODES`, the number `12` tells the software that there are altogether 12 nodes. It is then followed by a section of node coordinate information. Each node begins with a index number, then the x, y, and z coordinates. The keyword $ELEMENTS signals the begin of element information. Here we have six elements, with three prisms for the soil domain and three lines for the BHE compartment. Similar to the node information, each element begins with an index value, then the second index referring to the corresponding material

Table 2.1 Boundary heat fluxes q_{nTk} for different types of BHEs, reproduced after the FEFLOW book (Diersch 2014)

k	2U	1U	CXA	CXC
i1	$-\Phi_{fig}^{2U}(T_{g1}-T_{i1})$	$-\Phi_{fig}^{1U}(T_{g1}-T_{i1})$	$-\Phi_{fig}^{CXA}(T_{g1}-T_{i1})$	$-\Phi_{ff}^{CXC}(T_{o1}-T_{i1})$
			$-\Phi_{ff}^{CXA}(T_{o1}-T_{i1})$	
i2	$-\Phi_{fig}^{2U}(T_{g2}-T_{i2})$	–	–	–
o1	$-\Phi_{fog}^{2U}(T_{g3}-T_{o1})$	$-\Phi_{fog}^{1U}(T_{g2}-T_{o1})$	$-\Phi_{ff}^{CXA}(T_{i1}-T_{o1})$	$-\Phi_{fog}^{CXC}(T_{g1}-T_{o1})$
				$-\Phi_{ff}^{CXC}(T_{i1}-T_{o1})$
o2	$-\Phi_{fog}^{2U}(T_{g4}-T_{o2})$	–	–	–
g1	$-\Phi_{gs}^{2U}(T_s-T_{g1})$	$-\Phi_{gs}^{1U}(T_s-T_{g1})$	$-\Phi_{gs}^{CXC}(T_s-T_{g1})$	$-\Phi_{gs}^{CXA}(T_s-T_{g1})$
	$-\Phi_{fig}^{2U}(T_{i1}-T_{g1})$	$-\Phi_{fig}^{1U}(T_{i1}-T_{g1})$	$-\Phi_{fog}^{CXC}(T_{o1}-T_{g1})$	$-\Phi_{gs}^{CXA}(T_s-T_{g1})$
	$-\Phi_{gg2}^{2U}(T_{g2}-T_{g1})$	$-\Phi_{gg}^{1U}(T_{g2}-T_{g1})$	–	–
	$-\Phi_{gg1}^{2U}(T_{g3}-T_{g1})$			
	$-\Phi_{gg1}^{2U}(T_{g4}-T_{g1})$			
g2	$-\Phi_{gs}^{2U}(T_s-T_{g2})$	$-\Phi_{gs}^{1U}(T_s-T_{g2})$		
	$-\Phi_{fig}^{2U}(T_{i2}-T_{g2})$	$-\Phi_{fog}^{1U}(T_{o1}-T_{g2})$		
	$-\Phi_{gg2}^{2U}(T_{g1}-T_{g2})$	$-\Phi_{gg}^{1U}(T_{g1}-T_{g2})$	–	–
	$-\Phi_{gg1}^{2U}(T_{g3}-T_{g2})$			
	$-\Phi_{gg1}^{2U}(T_{g4}-T_{g2})$			
g3	$-\Phi_{gs}^{2U}(T_s-T_{g3})$			
	$-\Phi_{fig}^{2U}(T_{o1}-T_{g3})$			
	$-\Phi_{gg2}^{2U}(T_{g4}-T_{g3})$	–	–	–
	$-\Phi_{gg1}^{2U}(T_{g1}-T_{g3})$			
	$-\Phi_{gg1}^{2U}(T_{g2}-T_{g3})$			
g4	$-\Phi_{gs}^{2U}(T_s-T_{g4})$			
	$-\Phi_{fig}^{2U}(T_{o2}-T_{g4})$			
	$-\Phi_{gg2}^{2U}(T_{g3}-T_{g4})$	–	–	–
	$-\Phi_{gg1}^{2U}(T_{g1}-T_{g4})$			
	$-\Phi_{gg1}^{2U}(T_{g2}-T_{g4})$			

properties. The keywords `pris` and `line` denotes the type of the element, followed by the index of nodes that are connected to this element.

Listing 2.1 Mesh File

```
#FEM_MSH
$PCS_TYPE
HEAT_TRANSPORT_BHE
$NODES
12
0 0 0 0
1 0 1 0
2 1 0 0
3 0 1 1
4 0 0 1
5 1 0 1
6 0 1 2
7 0 0 2
8 1 0 2
9 0 1 3
```

```
10 0 0 3
11 1 0 3
$ELEMENTS
6
0 0 pris 2 1 0 5 3 4
1 0 pris 5 3 4 8 6 7
2 0 pris 8 6 7 11 9 10
3 1 line 9 6
4 1 line 6 3
5 1 line 3 1
#STOP
```

2.3.2 *Finite Element Discretization*

For the domain of BHEs, the governing Eqs. (2.5) and (2.7) are discretized by finite elements. By introducing the spatial weighting function ω, the weak statements write as

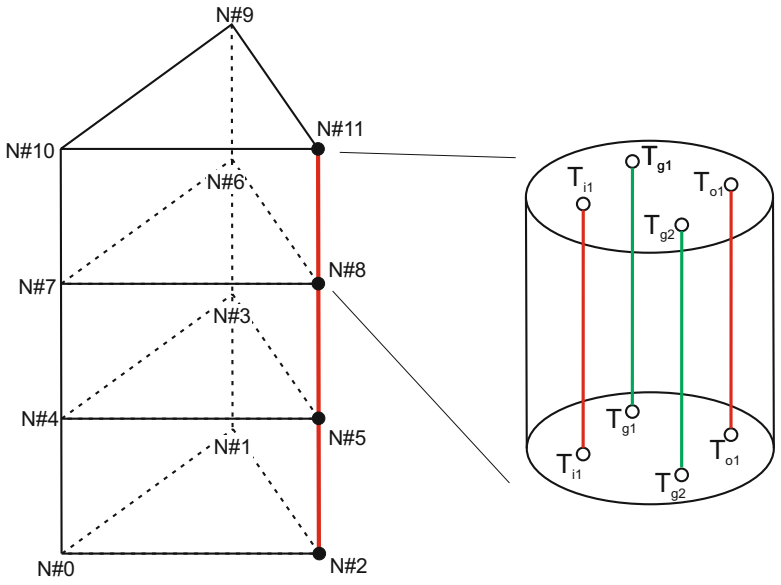

Fig. 2.2 Mesh and geometry structure, with soil domain represented by prism elements and BHE by line elements

Table 2.2 Different combination of primary variables for the borehole heat exchangers

Type of BHE	Number of primary variables	Combination of primary variables
1U	4	T_{i1}, T_{o1}, T_{g1}, T_{g2}
2U	8	T_{i1}, T_{i2}, T_{o1}, T_{o2}, T_{g1}, T_{g2}, T_{g3}, T_{g4}
CXA	3	T_{i1}, T_{o1}, T_{g1}
CXC	3	T_{i1}, T_{o1}, T_{g1}

$$\int_{\Omega_k}\left[\omega\rho^r c^r\left(\frac{\partial T_k}{\partial t}+\boldsymbol{u}\cdot\nabla T_k\right)+\nabla\omega\cdot(\Lambda^r\cdot\nabla T_k)\right]d\Omega=$$
$$-\int_{\Gamma_k}\omega q_{nT_k}d\Gamma_k+\int_{\Omega_k}\omega H_k d\Omega \text{ for k } = i1,\ o1,\ (i2,\ o2) \tag{2.8}$$

for the pipelines, and

$$\int_{\Omega_k}\left[\omega\rho^g c^g\frac{\partial T_k}{\partial t}+\nabla\omega\cdot(\Lambda^g\cdot\nabla T_k)\right]d\Omega=$$
$$-\int_{\Gamma_k}\omega q_{nT_k}d\Gamma_k+\int_{\Omega_k}\omega H_k d\Omega \quad \text{for k } = g1,\ (g2,\ (g3,\ g4)) \tag{2.9}$$

for the grout zones. If using Galerkin Finite Element Method (GFEM), the above Eqs. (2.8) and (2.9) can be written in the matrix form.

$$\boldsymbol{P}^{\pi}\cdot\dot{\boldsymbol{T}}^{\pi}+(\boldsymbol{L}^{\pi}+\boldsymbol{R}^{\pi})\cdot\boldsymbol{T}^{\pi}=\boldsymbol{W}^{\pi}-\boldsymbol{R}^{\pi s}\cdot\boldsymbol{T}^{s} \tag{2.10}$$

with the time derivative related mass matrix $\boldsymbol{P}^{\pi}$ formulated as

$$\boldsymbol{P}^{\pi}=\begin{cases}\begin{pmatrix}\boldsymbol{P}_{i1}&0&0&0&0&0&0&0\\0&\boldsymbol{P}_{i2}&0&0&0&0&0&0\\0&0&\boldsymbol{P}_{o1}&0&0&0&0&0\\0&0&0&\boldsymbol{P}_{o2}&0&0&0&0\\0&0&0&0&\boldsymbol{P}_{g1}&0&0&0\\0&0&0&0&0&\boldsymbol{P}_{g2}&0&0\\0&0&0&0&0&0&\boldsymbol{P}_{g3}&0\\0&0&0&0&0&0&0&\boldsymbol{P}_{g4}\end{pmatrix} & \text{2U}\\ \begin{pmatrix}\boldsymbol{P}_{i1}&0&0&0\\0&\boldsymbol{P}_{o1}&0&0\\0&0&\boldsymbol{P}_{g1}&0\\0&0&0&\boldsymbol{P}_{g2}\end{pmatrix} & \text{1U}\\ \begin{pmatrix}\boldsymbol{P}_{i1}&0&0\\0&\boldsymbol{P}_{o1}&0\\0&0&\boldsymbol{P}_{g1}\end{pmatrix} & \text{CXA or CXC.}\end{cases} \tag{2.11}$$

For the pipeline or grout zone of the BHE, the mass matrix writes

$$\boldsymbol{P}_k=\begin{cases}\Sigma_e\int_{\Omega_k^e}\rho^r c^r N_i N_j d\Omega^e & \text{for } k=i1,o1,(i2,o2)\\ \Sigma_e\int_{\Omega_k^e}\rho^g c^g N_i N_j d\Omega^e & \text{for } k=g1,(g2,(g3,g4)).\end{cases} \tag{2.12}$$

The heat exchange terms are summarized in the matrix $\boldsymbol{R}^{\pi}$,

$$
\boldsymbol{R}^{\pi} = \begin{cases}
\begin{pmatrix}
\boldsymbol{R}_{i1}+\boldsymbol{R}_{io} & 0 & -\boldsymbol{R}_{io} & 0 & -\boldsymbol{R}_{i1} & 0 & 0 & 0 \\
0 & \boldsymbol{R}_{i2} & 0 & 0 & 0 & -\boldsymbol{R}_{i2} & 0 & 0 \\
-\boldsymbol{R}_{io} & 0 & \boldsymbol{R}_{io}+\boldsymbol{R}_{o1} & 0 & 0 & 0 & -\boldsymbol{R}_{o1} & 0 \\
0 & 0 & 0 & \boldsymbol{R}_{o2} & 0 & 0 & 0 & -\boldsymbol{R}_{o2} \\
-\boldsymbol{R}_{i1} & 0 & 0 & 0 & \boldsymbol{R}_{i1}+2\boldsymbol{R}_{g1}+\boldsymbol{R}_{g2}+\boldsymbol{R}_{s} & -\boldsymbol{R}_{g2} & -\boldsymbol{R}_{g1} & -\boldsymbol{R}_{g1} \\
0 & -\boldsymbol{R}_{i2} & 0 & 0 & -\boldsymbol{R}_{g2} & \boldsymbol{R}_{i2}+2\boldsymbol{R}_{g1}+\boldsymbol{R}_{g2}+\boldsymbol{R}_{s} & -\boldsymbol{R}_{g1} & -\boldsymbol{R}_{g1} \\
0 & 0 & -\boldsymbol{R}_{o1} & 0 & -\boldsymbol{R}_{g1} & -\boldsymbol{R}_{g1} & \boldsymbol{R}_{o1}+2\boldsymbol{R}_{g1}+\boldsymbol{R}_{g2}+\boldsymbol{R}_{s} & 0 \\
0 & 0 & 0 & -\boldsymbol{R}_{o2} & -\boldsymbol{R}_{g1} & -\boldsymbol{R}_{g1} & -\boldsymbol{R}_{g2} & \boldsymbol{R}_{o2}+2\boldsymbol{R}_{g1}+\boldsymbol{R}_{g2}+\boldsymbol{R}_{s}
\end{pmatrix} & \text{2U} \\
\begin{pmatrix}
\boldsymbol{R}_{i1}+\boldsymbol{R}_{io} & -\boldsymbol{R}_{io} & -\boldsymbol{R}_{i1} & 0 \\
-\boldsymbol{R}_{io} & \boldsymbol{R}_{o1}+\boldsymbol{R}_{io} & 0 & -\boldsymbol{R}_{o1} \\
-\boldsymbol{R}_{i1} & 0 & \boldsymbol{R}_{i1}+\boldsymbol{R}_{g1} & -\boldsymbol{R}_{g1} \\
0 & -\boldsymbol{R}_{o1} & -\boldsymbol{R}_{g1} & \boldsymbol{R}_{o1}+\boldsymbol{R}_{g1}
\end{pmatrix} & \text{1U} \\
\begin{pmatrix}
\boldsymbol{R}_{i1}+\boldsymbol{R}_{io} & -\boldsymbol{R}_{io} & -\boldsymbol{R}_{i1} \\
-\boldsymbol{R}_{io} & \boldsymbol{R}_{io} & 0 \\
-\boldsymbol{R}_{i1} & 0 & \boldsymbol{R}_{i1}
\end{pmatrix} & \text{CXA} \\
\begin{pmatrix}
\boldsymbol{R}_{io} & -\boldsymbol{R}_{io} & 0 \\
-\boldsymbol{R}_{io} & \boldsymbol{R}_{io}+\boldsymbol{R}_{o1} & -\boldsymbol{R}_{o1} \\
0 & -\boldsymbol{R}_{o1} & \boldsymbol{R}_{o1}
\end{pmatrix} & \text{CXA}
\end{cases}
\tag{2.13}
$$

$$\boldsymbol{L}^{\pi} = \begin{cases} \begin{pmatrix} \boldsymbol{L}_{i1} & 0 & 0 & 0 & 0 & 0 & 0 & 0 \\ 0 & \boldsymbol{L}_{i2} & 0 & 0 & 0 & 0 & 0 & 0 \\ 0 & 0 & \boldsymbol{L}_{o1} & 0 & 0 & 0 & 0 & 0 \\ 0 & 0 & 0 & \boldsymbol{L}_{o2} & 0 & 0 & 0 & 0 \\ 0 & 0 & 0 & 0 & \boldsymbol{L}_{ig} & 0 & 0 & 0 \\ 0 & 0 & 0 & 0 & 0 & \boldsymbol{L}_{ig} & 0 & 0 \\ 0 & 0 & 0 & 0 & 0 & 0 & \boldsymbol{L}_{og} & 0 \\ 0 & 0 & 0 & 0 & 0 & 0 & 0 & \boldsymbol{L}_{og} \end{pmatrix} & \text{2U} \\ \begin{pmatrix} \boldsymbol{L}_{i1} & 0 & 0 & 0 \\ 0 & \boldsymbol{L}_{o1} & 0 & 0 \\ 0 & 0 & \boldsymbol{L}_{g1} & 0 \\ 0 & 0 & 0 & \boldsymbol{L}_{g2} \end{pmatrix} & \text{1U} \\ \begin{pmatrix} \boldsymbol{L}_{i1} & 0 & 0 \\ 0 & \boldsymbol{L}_{o1} & 0 \\ 0 & 0 & \boldsymbol{L}_{g1} \end{pmatrix} & \text{CXA or CXC} \end{cases} \tag{2.14}$$

For the pipeline part, the transport operator L is composed of both advection and dispersion terms,

$$\boldsymbol{L}_k = \Sigma_e \int_{\Omega_k^e} \left(N_i \rho^r c^r \nabla N_j + \nabla N_i \cdot (\Lambda \cdot \nabla N_j) \right) d\Omega^e \quad \text{for} \quad k = i1, o1, (i2, o2). \tag{2.15}$$

While for the grout zones, only the heat dissipation terms contribute

$$\boldsymbol{L}_{ig} = \boldsymbol{L}_{og} = \Sigma_e \int_{\Omega_k^e} \nabla N_i \cdot (\Lambda^g \cdot \nabla N_j) d\Omega^e \quad \text{for} \quad k = (g1, g2, g3, g4). \tag{2.16}$$

For the source and sink terms,

$$\boldsymbol{W}_k = \Sigma_e \int_{\Omega_k^e} N_i H_k d\Omega^e \quad \text{for} \quad \forall k. \tag{2.17}$$

For the heat exchange terms $\boldsymbol{R}_{\pi s}$ and $\boldsymbol{R}_{s\pi}$,

$$\boldsymbol{R}^{s\pi} = \boldsymbol{R}^{\pi s T} = \begin{cases} (\boldsymbol{0}\ \boldsymbol{0}\ \boldsymbol{0}\ \boldsymbol{0}\ -\boldsymbol{R}_s\ -\boldsymbol{R}_s\ -\boldsymbol{R}_s\ -\boldsymbol{R}_s) & \text{2U} \\ (\boldsymbol{0}\ \boldsymbol{0}\ -\boldsymbol{R}_s\ -\boldsymbol{R}_s) & \text{1U} \\ (\boldsymbol{0}\ \boldsymbol{0}\ -\boldsymbol{R}_s) & \text{CXA or CXC} \end{cases} \tag{2.18}$$

2.3.3 Assembly of the Global Equation System

In order to simulate the heat transfer between BHEs and the surrounding soil, the governing equations for the pipeline and grout zones must be assemble into a global

matrix system together with the linearized heat transport equation of the soil. When the Eq. (2.10) is combined with the matrix form of Eq. (2.3), the global matrix system writes as

$$\begin{pmatrix} \boldsymbol{P}^s & \boldsymbol{0} \\ \boldsymbol{0} & \boldsymbol{P}^\pi \end{pmatrix} \cdot \begin{pmatrix} \dot{\boldsymbol{T}}^s \\ \dot{\boldsymbol{T}}^\pi \end{pmatrix} + \begin{pmatrix} \boldsymbol{L}^s - \boldsymbol{R}^\pi & \boldsymbol{R}^{s\pi} \\ \boldsymbol{R}^{\pi s} & \boldsymbol{T}^\pi \end{pmatrix} \cdot \begin{pmatrix} \boldsymbol{T}^s \\ \boldsymbol{T}^\pi \end{pmatrix} = \begin{pmatrix} \boldsymbol{W}^s \\ \boldsymbol{W}^\pi \end{pmatrix}. \tag{2.19}$$

When Euler time discretization is applied on the above equation, the fully linearized global matrix system looks like

$$\begin{pmatrix} \boldsymbol{A}^s & \boldsymbol{R}^{s\pi} \\ \boldsymbol{R}^{s\pi} & \boldsymbol{A}^\pi \end{pmatrix} \cdot \begin{pmatrix} \boldsymbol{T}^s \\ \boldsymbol{T}^\pi \end{pmatrix}_{n+1} = \begin{pmatrix} \boldsymbol{B}^s \\ \boldsymbol{B}^\pi \end{pmatrix}_{n+1,n}, \tag{2.20}$$

where n and $n+1$ represents the previous and current time step. If a corrector recurrence scheme is applied, then the left-hand-side matrix and right-hand-side vectors writes as

$$\begin{aligned} \boldsymbol{A}^s &= \frac{1}{\Delta t_n}\boldsymbol{P}^s + \theta\,(\boldsymbol{L}^s - \boldsymbol{R}^\pi) \\ \boldsymbol{B}^s &= \left(\frac{1}{\Delta t_n}\boldsymbol{P}^s - (1-\theta)\,(\boldsymbol{L}^s - \boldsymbol{R}^\pi)\right) \cdot \boldsymbol{T}^s_n + \boldsymbol{W}^s_{n+1}\theta + \boldsymbol{W}^s_n(1-\theta) \\ \boldsymbol{A}^\pi &= \frac{1}{\Delta t_n}\boldsymbol{P}^\pi + \theta\boldsymbol{L}^\pi \\ \boldsymbol{B}^\pi &= \left(\frac{1}{\Delta t_n}\boldsymbol{P}^\pi - (1-\theta)\boldsymbol{L}^\pi\right) \cdot \boldsymbol{T}^\pi_n + \boldsymbol{W}^\pi_{n+1}\theta + \boldsymbol{W}^\pi_n(1-\theta) \end{aligned} \tag{2.21}$$

2.3.4 Picard Iterations and Time Stepping Schemes

After the $\boldsymbol{A}$ matrices and $\boldsymbol{B}$ vectors have been assembled, the OpenGeoSys software employs a linear solver to calculate the temperatures $\boldsymbol{T}$ for the new time step, based on the previous time step value. Notice that, the heat exchange coefficients $\boldsymbol{R}^{s\pi}$ and $\boldsymbol{R}^{\pi s}$ will be multiplied with the temperature values, and producing the heat exchange flux between the soil and the BHE domain. This term is linearly dependent on the temperature difference. However, when a new set of temperature values are produced, the heat flux changes respectively. Therefore, a Picard iteration scheme has to be employed by the OpenGeoSys software, to solve for a set of converged temperature values. The following log message from a typical simulation demonstrates the Picard iteration behavior.

Listing 2.2 Log File of A Simulation Run

```
============================================
->Process 1: HEAT_TRANSPORT_BHE
============================================
PCS non-linear iteration: 0/2
Assembling equation system...
Calling linear solver...
SpBICGSTAB iteration: 2/1000
-->End of PICARD iteration: 0/2
PCS error: 0.00110317
->Euclidian norm of unknowns: 0.00596578
PCS non-linear iteration: 1/2
Assembling equation system...
Calling linear solver...
SpBICGSTAB iteration: 2/1000
-->End of PICARD iteration: 1/2
PCS error: 1.37569e-006
->Euclidian norm of unknowns: 1.82299e-005
This step is accepted.
Data output: Polyline profile - BHE_1
############################################################
```

As can be found in the log file, one iteration of the HEAT_TRANSPORT_BHE process is needed. In this example, the tolerance of Picard iteration is set to 1.0×10^{-4}, and the simulation will normally converge after one iteration.

In the work of Diersch et al. (2011a); Diersch (2014), they suggested to inverse the matrix system for BHE domain separately, then integrate its influence into the soil domain by a *Schur complement* operation. Such procedures is reasonable as the BHE domain is typically small (degree of freedom number in the order of thousands by thousands). However, non-linearity of the governing equations cannot be eliminated without an iteration step. Their test run also shows that at least one iteration is necessary to obtain the accurate temperature values. Considering only little effort is added to the linear solver, we choose to directly iterate the linearized matrix system of Eq. (2.21). Our simulation shows that convergence can be achieve after one Picard iteration in nearly all simulations.

Normally at the beginning of the simulation, when refrigerant starts flowing in the pipeline, the temperature change in the grout and soil is relatively large. This makes the model very difficult to converge, i.e. more than dozens of Picard iterations are required. It is then suggested to specify a small time step size in terms of minutes for the beginning stage of the simulation. Once the flow and heat transport is stabilized, a larger time step size can then be taken by the model.

Chapter 3
OGS Project: Simulating Heat Transport Model with BHEs

3.1 Download and Compile the Source Code

Since OpenGeoSys is an open-source project, users can download the source code from the following website and build the binary executable file by themselves.

https://github.com/ufz/ogs5

For different platforms, i.e. Windows, Mac or Linux, the general procedure of building an OGS executable and running a model simulation would be very similar. Here in this chapter, such process will be demonstrated based on a Windows operation system. It will be shown step by step, how to build the source code and construct a simple model with one borehole heat exchanger in the middle of the model domain.

3.1.1 Download the Source Code

Assuming the Git command line interface has already been installed on the system, the OGS source code can be obtained by typing in the command line prompt the following content.

Listing 3.1 Downloading the source code with Git

```
C:\haibing_working\ogs>git clone https://github.com/ufz/ogs5.git
```

Or, if one prefers a graphical interface, it is recommend to use SourceTree on the Windows platform. After a fresh installation of the software SourceTree, the following interface will appear (Fig. 3.1). By clicking the button Clone/New in the upper-left corner, one will be asked to give the location of repository. You may use the Github link provided above, or first fork from the above repository and clone

H. Shao et al., *Geoenergy Modeling II*, SpringerBriefs in Energy,
DOI 10.1007/978-3-319-45057-5_3

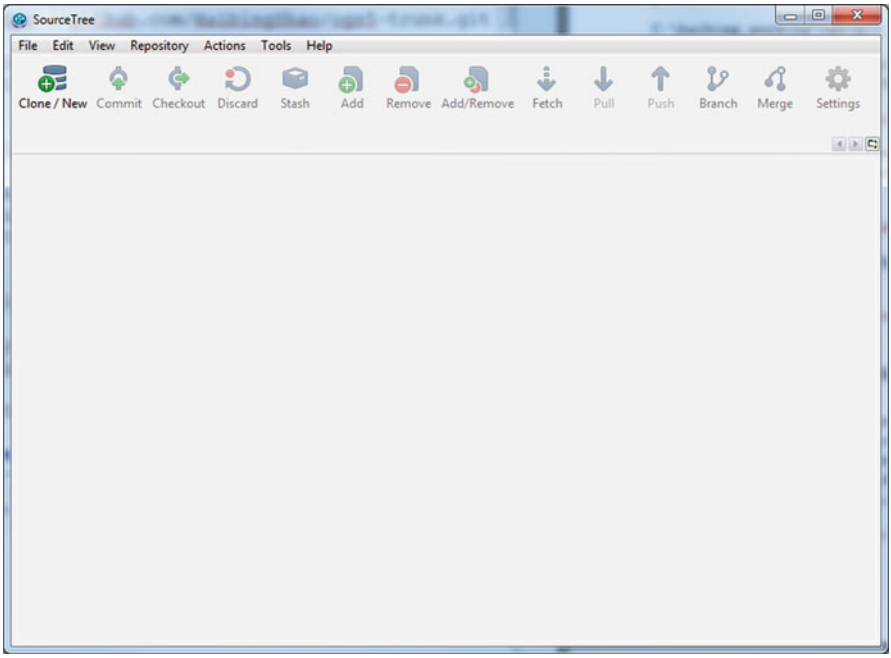

Fig. 3.1 SourceTree window as in the initial stage

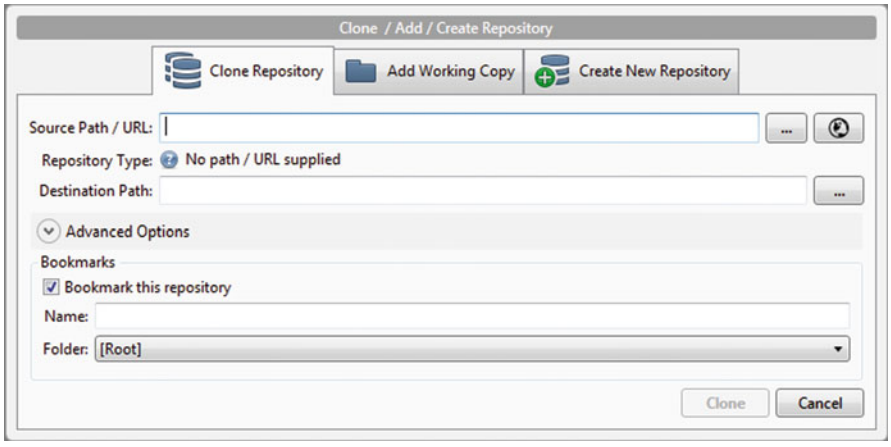

Fig. 3.2 SourceTree dialog asking for the location of the repository

from your own repository on Github (Fig. 3.2). After the code has been successfully cloned to a local drive, one can see all the history of code development in SourceTree as shown in Fig. 3.3.

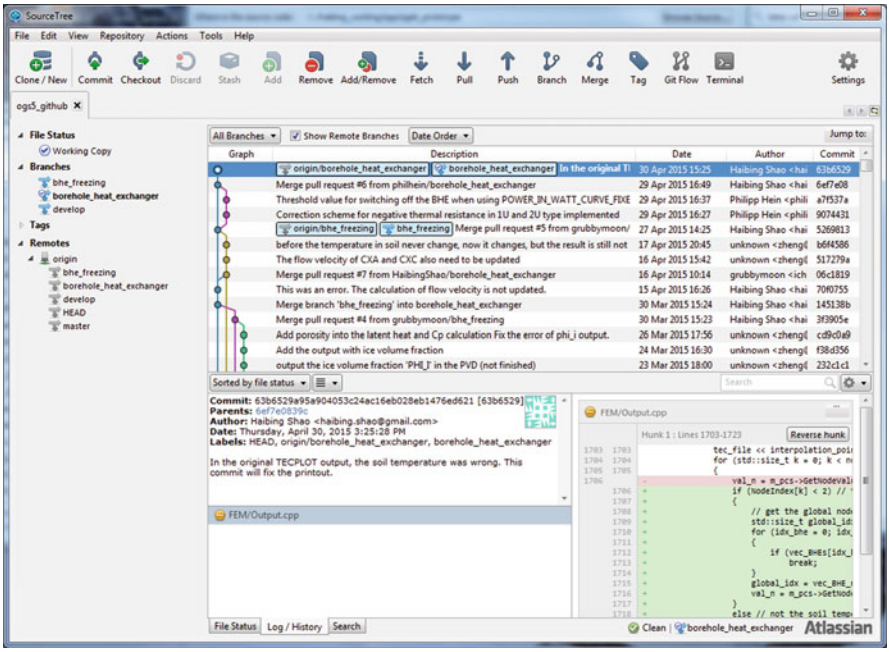

Fig. 3.3 SourceTree window with detailed history of a repository

3.1.2 Using CMake to Configure the Building Project

Before the compilation of the source code, the software CMake needs to be employed to generate the configuration and makefiles which are specific to the building environment. Here the CMake version 2.8.12.2 is employed for demonstration. In Fig. 3.4, CMake GUI was freshly started. First, one needs to define two paths in the CMake GUI. The first one is the folder where the source code of OGS is located. The second path refers to the folder where the makefiles will be generated. After clicking on the "Configure" button, CMake will ask several questions, depending on different types of operating system and the compiling tools. In this example, the "Visual Studio 2013 x86" option was chosen. Once the configuration has finished, the build options will be shown in the CMake GUI. To build the OpenGeoSys code with BHE features, one only needs to choose the option `OGS_FEM`. By clicking on the "Generate" button, CMake will prepare all makefiles in the build folder (Fig. 3.5).

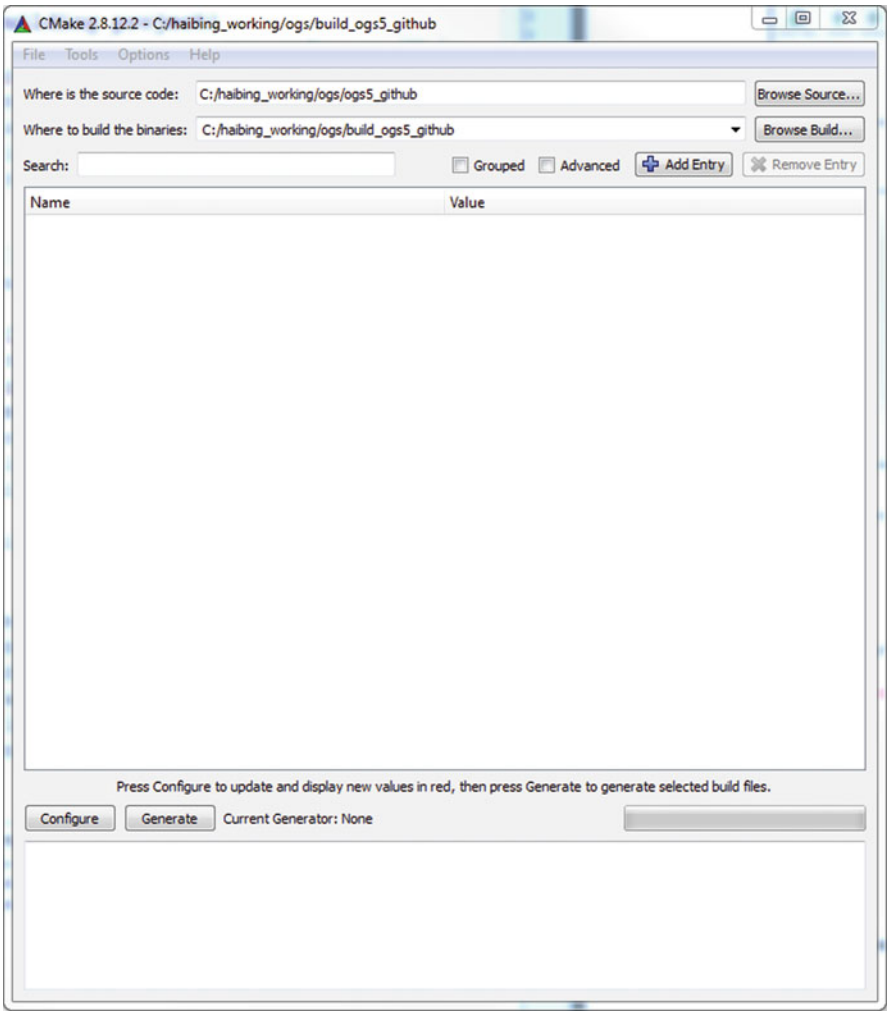

Fig. 3.4 CMake interface of configuring the build information

3.1.3 Compiling the Code

As the author is mainly developing the code with Microsoft Visual Studio, the building process will be demonstrated with the same software. Provided the configuration was accomplished by CMake successfully in the previous step, there will be a file named with "OGS.sln" in the build folder. By opening this Visual Studio solution

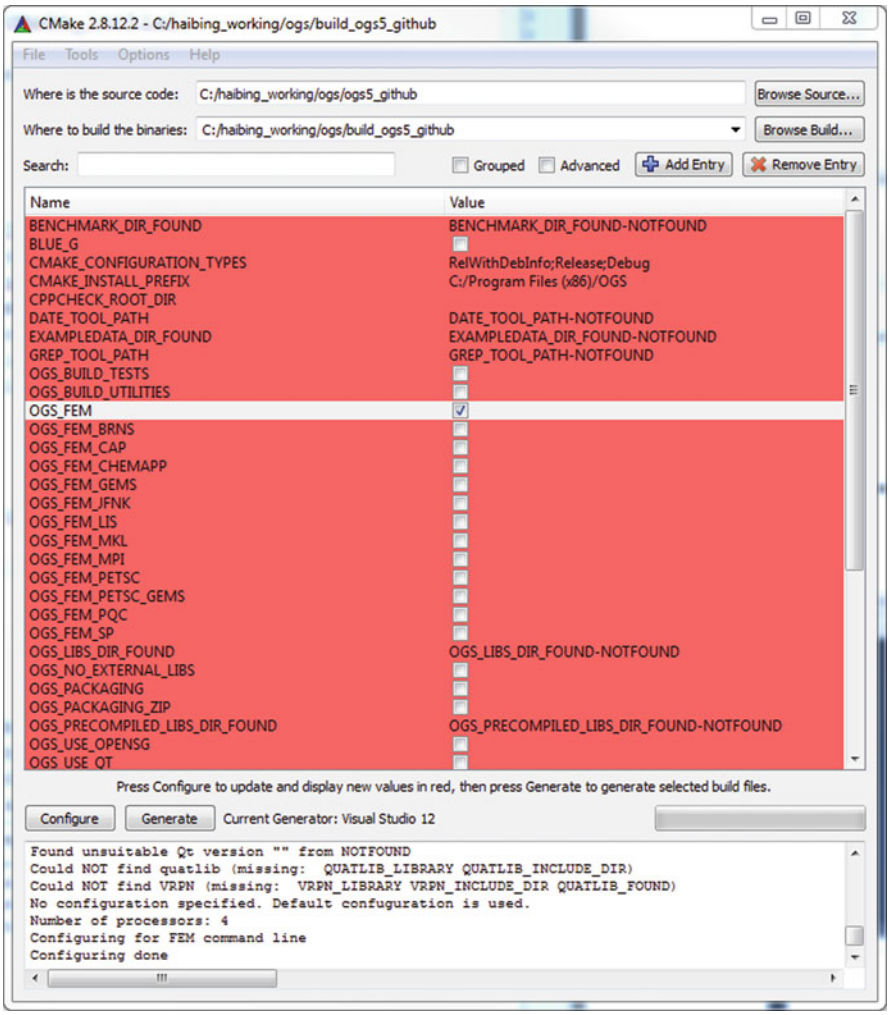

Fig. 3.5 CMake interface showing different building options

file, the source code will be loaded into the development environment along with all the building configurations (Fig. 3.6). To build the source code, just choose from the menu "BUILD", and then click on the first option "Build Solution". It takes a couple of minutes to run the full building process for the first time. After the building is completed, an executable file "ogs.exe" can be found under the "bin" folder and then "Debug" or "Release" folder, depending on which building mode has been adopted.

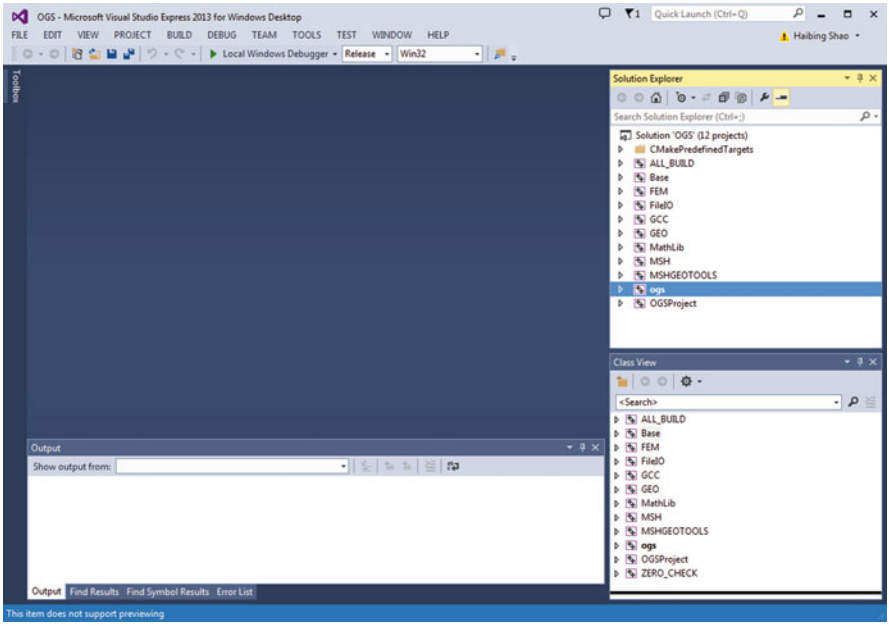

Fig. 3.6 Visual Studio interface after opening the OpenGeoSys solution file

3.2 Define Heat Transport Process with BHEs

In the last section, the OGS code was successfully compiled and an ogs.exe executable file has been built. In this section, a modelling project will be established to simulate the heat transport process with borehole heat exchangers.

3.2.1 Process Definition

Originally, the heat transport simulation in an OpenGeoSys project is performed by defining the process as `HEAT_TRANSPORT`. To include the interaction with BHEs, a new process has been introduced and named as "`HEAT_TRANSPORT_BHE`". The model input files bear the name "project_name.ext_name". The "project_name" is a unique string defined by the user to identify a project. The "ext_name" are pre-defined extensions which refers to a particular type of input configuration. In the following, a PCS file is first introduced, with one `GROUNDWATER_FLOW` and one `HEAT_TRANSPORT_BHE` process defined in it. If the project is named as "bhe_test", then the PCS file should be named as "bhe_test.pcs". Its content is shown in the following text box.

Listing 3.2 PCS File Definition including Interaction with Borehole Heat Exchangers

```
#PROCESS
$PCS_TYPE
  GROUNDWATER_FLOW
$DEACTIVATED_SUBDOMAIN
  1
  1
#PROCESS
 $PCS_TYPE
   HEAT_TRANSPORT_BHE
 $PRIMARY_VARIABLE
   TEMPERATURE_SOIL
#STOP
```

3.2.2 Deactivated Sub-domains

In the above PCS file, some readers might have already noticed that there are two numbers given under the key word `$DEACTIVATED_SUBDOMAIN`. The first number "1" on line #7 means there is one sub-domain deactivated for the `GROUNDWATER_FLOW` process, and the second number "1" on line #8 identifies the index of this deactivated domain. So why does the sub-domain "1" need to be turned off? This is because the sub-domain "0" in this project is referring to the soil domain, while the sub-domain "1" is the borehole heat exchanger compartment. Since the BHE is grouted and impermeable, it is not necessary to calculate groundwater flow through a BHE. Therefore its representative sub-domain is deactivated.

3.2.3 Primary Variables

In Sects. 2.1 and 2.2, it has been introduced that there are multiple primary variables applied in the BHE simulation. In the soil sub-domain primary variable is the soil temperature, while on the BHE they are the temperatures of inlet outlet pipes and the surrounding grout zones. The key words used for these processes, are summarized in Table 3.1. In Sect. 3.8, when the output is specified, these key words will be used.

3.3 Geometry of BHEs

Listing 3.3 Geometry Definition in the GLI File of an OpenGeoSys Project

```
#POINTS
0  0.0 0.0  18.32 $NAME POINT0
1  1.8 0.0  18.32 $NAME POINT1
2  1.8 1.8  18.32 $NAME POINT2
```

Table 3.1 Key words used in OGS BHE project for different primary variables

Symbols	Key words	Meaning
T_s	TEMPERATURE_SOIL	Soil temperature
T_{i1}	TEMPERATURE_IN_1	Inflow temperature (1U, CXC, CXA)
T_{i2}	TEMPERATURE_IN_2	Inflow temperature (2U)
T_{o1}	TEMPERATURE_OUT_1	Outflow temperature (1U, CXC, CXA)
T_{o2}	TEMPERATURE_OUT_2	Outflow temperature (2U)
T_{g1}	TEMPERATURE_G_1	Temperature of grout zone 1
T_{g2}	TEMPERATURE_G_2	Temperature of grout zone 2
T_{g3}	TEMPERATURE_G_3	Temperature of grout zone 3
T_{g4}	TEMPERATURE_G_4	Temperature of grout zone 4

```
3   0.0 1.8   18.32 $NAME POINT3
4   0.9 0.9   18.32 $NAME POINT4
5   0.0 0.0   0.0   $NAME POINT5
6   1.8 0.0   0.0   $NAME POINT6
7   1.8 1.8   0.0   $NAME POINT7
8   0.0 1.8   0.0   $NAME POINT8
9   0.9 0.9   0.0   $NAME POINT9
10 1.14 0.9   18.32 $NAME POINT10
11 1.14 0.9   0.0   $NAME POINT11
12 1.34 0.9   18.32 $NAME POINT12
13 1.34 0.9   0.0   $NAME POINT13
14 1.55 0.9   18.32 $NAME POINT14
15 1.55 0.9   0.0   $NAME POINT15
16 1.75 0.9   18.32 $NAME POINT16
17 1.75 0.9   0.0   $NAME POINT17
#POLYLINE
$NAME
BHE_1
$POINTS
4
9
#STOP
```

As shown in the GLI file above, "BHE_1" is referring to a polyline starting from point #4 and ending until point #9. To define different BHEs, each BHE in the model has to be given a different polyline in the geometry definition. The geometry names will be used afterwards in the MMP and OUT file as a reference to differentiate the BHEs.

3.4 Mesh of BHEs

In Sect. 2.3.1, it has been already introduced that the BHEs are treated in the OGS model as a second domain. Generally, the soil matrix is meshed with 3D prism elements. In comparison to standard mesh file, the location of all mesh nodes remains the same, while additional 1D elements are added at the end of the element section, to represent the BHEs.

Listing 3.4 The Element Section in MSH File

```
$ELEMENTS
155062
0 0 pris 1673 1582 1671 598 507 596
...
14650 0 pris 7627 7614 7541 6552 6539 6466
14651 1 pris 9198 9107 9196 8123 8032 8121
...
23022 1 pris 11927 11914 11841 10852 10839 10766
23023 2 pris 13498 13407 13496 12423 12332 12421
...
56510 2 pris 29127 29114 29041 28052 28039 27966
56511 3 pris 30698 30607 30696 29623 29532 29621
...
154881 3 pris 79652 79639 79566 78577 78564 78491
154882 4 line 4 1079
...
154926 4 line 47304 48379
154927 5 line 5 1080
...
154971 5 line 47305 48380
154972 6 line 6 1081
...
155016 6 line 47306 48381
155017 7 line 7 1082
...
155061 7 line 47307 48382
#STOP
```

In the mesh file, different BHEs are marked with different material group indices. Taking the above mesh file as an example, the first number in each row denotes the index of the element. After that comes the index of the material group. In this project, there are all together eight material groups, with the index from 0 to 7. The material group #0, #1, #2 and #3 refers to the four soil layers in the simulation domain. That is why they are meshed with 3D prism elements. For the material group #4, #5, #6 and #7, each of them represents a BHE, which is meshed with 1D line elements. Since different BHEs might have different configurations, such as the depth, U-tube diameters, and flow rates etc., these BHE parameters are given as part of the material group definition in the MMP file. In Chap. 4, introduction will be given regarding how to use a meshing tool to generate the mesh file.

3.5 Parameters of BHEs

The parameters of the borehole heat exchangers are listed in the MMP file. In the following text box, an example was given. For each BHE, a unique MMP record needs to be given, starting with the key word "#MEDIUM_PROPERTIES". Under the key word "$GEO_TYPE", the corresponding polyline was given, identifying the location of this BHE. Following the key word "$BOREHOLE_HEAT_EXCHANGER", more specific information was defined, such as the length of the BHE, borehole diameter, refrigerant flow rate etc. Most of the key words applied here are self-explanatory. A more detailed definition is listed in Table 3.2.

Table 3.2 Parameters of BHE configuration available in the MMP file

Key words	Value to fill	Unit	Default value	Remarks
BHE_TYPE	BHE_TYPE_1U BHE_TYPE_2U BHE_TYPE_CXA BHE_TYPE_CXC	–		Specify the type of BHE
BHE_BOUNDARY_TYPE	FIXED_INFLOW_TEMP FIXED_INFLOW_TEMP_CURVE POWER_IN_WATT POWER_IN_WATT_CURVE_FIXED_DT POWER_IN_WATT_CURVE_FIXED_FLOW_RATE FIXED_TEMP_DIFF	–		Different boundary conditions for the BHE
BHE_POWER_IN_WATT_VALUE	Double number	W		A fixed power value Positive means heating the BHE, Negative means cooling
BHE_POWER_IN_WATT_CURVE_IDX	Integer number	–		Index of curve in the RFD file
BHE_DELTA_T_VALUE	Double number	K		Only when the boundary type FIXED_TEMP_DIFF is chosen
BHE_SWITCH_OFF_THRESHOLD	Double number	K		
BHE_LENGTH	Double number	m		Length of the BHE
BHE_DIAMETER	Double number	m		Diameter of the borehole
BHE_REFRIGERANT_FLOW_RATE	Double number	m^3/s		Flow rate of circulating refrigerant inside the pipeline of the BHE
BHE_INNER_RADIUS_PIPE	Double number	m		Inner radius of the pipe
BHE_OUTER_RADIUS_PIPE	Double number	m		Outer radius of the pipe
BHE_PIPE_IN_WALL_THICKNESS	Double number	m		Inlet pipe wall thickness
BHE_PIPE_OUT_WALL_THICKNESS	Double number	m		Outlet pipe wall thickness
BHE_FLUID_TYPE	Integer number	m		Index of fluid defined in the MFP file

Listing 3.5 Definition of BHE parameters in MMP File

```
; properties of BHE 1
#MEDIUM_PROPERTIES
 $GEO_TYPE
   POLYLINE BHE_1
 $BOREHOLE_HEAT_EXCHANGER
   BHE_TYPE
     BHE_TYPE_1U
   BHE_BOUNDARY_TYPE
     POWER_IN_WATT_CURVE_FIXED_FLOW_RATE  ;
   BHE_POWER_IN_WATT_CURVE_IDX
     1
   BHE_LENGTH
     46
   BHE_DIAMETER
     0.15
   BHE_REFRIGERANT_FLOW_RATE
     9.17E-05
   BHE_INNER_RADIUS_PIPE
     0.0131
......
```

One parameter that needs further explanation is the boundary condition that will be imposed on a BHE. In most cases, the inflow temperature of the BHE is controlled by the operation logic of the heat pump, and subsequently by the thermal load from the building. Therefore, several different types of BHE boundary conditions have been provided in the MMP files.

- FIXED_INFLOW_TEMP
  This is the simplest case, where the BHE inflow temperature is a constant over the simulation period. Such kind of boundary condition is rarely used for real scenario analysis, but for testing and benchmark purposes it is kept in the configuration.
- FIXED_INFLOW_TEMP_CURVE
  With this type of boundary condition, the BHE inflow temperature is specified according to a time dependent curve, which is defined in the RFD file. An example of time dependent curve can be found in one of the benchmark cases (Sect. 5.2).
- FIXED_TEMP_DIFF
  Some heat pump adopt an operation logic, which impose a fixed temperature difference between the inflow and outflow from the BHE. When this type of boundary condition is specified, the numerical model will first check the outflow temperature, and then calculate the inflow temperature by adding this ΔT value.
- POWER_IN_WATT
  This type of boundary configuration will specify the amount of power withdrawn or injected through the BHE. In the former case, there will be a negative value, and in the latter one a positive number. Through the simulation, the program will divide this power value by the product of fluid heat capacity, fluid density and the flow rate. The resultant ΔT value will then be added on the outflow temperature, through which the inflow temperature is determined. Such calculation will be performed before each iteration of the linear equation solution.

- POWER_IN_WATT_CURVE_FIXED_DT
  In this scenario, the BHE thermal load is specified according to a predefined curve in the RFD file. Meanwhile, a fixed ΔT values will be maintained, i.e. the flow rate will be dynamically calculated based on the thermal load, the circulating fluid properties, and the given ΔT value. If the resultant flow rate is below a certain threshold (by default $1.0 \times 10^{-6}\,\mathrm{m}^3/\mathrm{s}$, the program will assume that the heat pump and fluid circulation is switched off.
- POWER_IN_WATT_CURVE_FIXED_FLOW_RATE
  Different from the previous configuration, this type of boundary will maintain a fixed flow rate instead of ΔT. In this case the ΔT value will be dynamically calculated using the same relationship, while the flow rate is kept the same.
- BHE_BOUND_BUILDING_POWER_IN_WATT_CURVE_FIXED_DT
  and
  BHE_BOUND_BUILDING_POWER_IN_WATT_CURVE_FIXED_FLOW_RATE
  The additional feature in these two types of boundary is the inclusion of heat pump efficiency. Conventionally, this efficiency value is quantified by the coefficient of performance (COP) Casasso and Sethi (2014)

$$COP = \frac{\dot{Q}}{W} \tag{3.1}$$

where $\dot{Q}$ is the amount of thermal power required by the building, and W is the electricity consumed by the heat pump. The COP can be determined by the temperature of circulating fluid at the BHE outlet, and the temperature required at the heating end [see Jaszczur and Śliwa (2013) and also Eq. (3.2)]. Although there are other factors influencing the heat pump COP, it is widely assumed that the COP is linearly dependent on the BHE outflow temperature. The same simplification can be found in e.g. Kahraman and Çelebi (2009), Casasso and Sethi (2014) and Sanner et al. (2003). The COP of a typical heat pump can be approximated by the following relationship,

$$COP = a + bT_{out} \tag{3.2}$$

where the parameters a and b is can be defined in the MMP file.

In reality, the thermal load of the BHE $\dot{Q}_{BHE}$ is not the same as the building heat demand $\dot{Q}_{Building}$ (see e.g. Casasso and Sethi 2014; Eicker and Vorschulze 2009; Speer 2005). To shift the heat from the ground to the building, the heat pump needs about 20–30 % of the energy in the form of electricity. This amount of heat must be subtracted from the thermal load.

$$\dot{Q}_{BHE} = \dot{Q}_{Building}\frac{COP - 1}{COP} \tag{3.3}$$

This effect will be explicitly considered by these two boundary conditions. With these two configurations, the building thermal load is specified. During the

model simulation, the COP of the heat pump will be dynamically calculated by OGS, and the amount of BHE thermal load will be updated accordingly.

3.6 Initial Conditions for the BHE

In the IC file, initial temperatures on different compartments of the BHE have to be given, together with temperatures of the soil at the beginning of the simulation. The following example shows that the initial temperature of the soil, of the inlet and outlet pipeline are all set to be 22 °C. Notice that the initial condition must be imposed also on the two grout zones surrounding the pipelines.

Listing 3.6 The Initial Condition Configuration

```
#INITIAL_CONDITION
 $PCS_TYPE
  HEAT_TRANSPORT_BHE
 $PRIMARY_VARIABLE
  TEMPERATURE_SOIL
 $GEO_TYPE
  DOMAIN
 $DIS_TYPE
  CONSTANT  22.0

#INITIAL_CONDITION
 $PCS_TYPE
  HEAT_TRANSPORT_BHE
 $PRIMARY_VARIABLE
  TEMPERATURE_IN_1
 $GEO_TYPE
  POLYLINE BHE_1
 $DIS_TYPE
  CONSTANT  22.0

#INITIAL_CONDITION
 $PCS_TYPE
  HEAT_TRANSPORT_BHE
 $PRIMARY_VARIABLE
  TEMPERATURE_OUT_1
 $GEO_TYPE
  POLYLINE BHE_1
 $DIS_TYPE
  CONSTANT  22.0
...
```

It is very often that the shallow subsurface has a natural geothermal gradient. In this case, the initial temperature of the soil can be specified to gradually increase along with the depth. The following example shows how to define such a case. There are three values after the keyword GRADIENT. The first values is the reference depth. The second one is the temperature value at this depth, and the third one is the geothermal gradient in the z-direction. In this example, the soil temperature was specified to be 13.32 °C at −120 m, and has a gradient of 0.016 K m^{-1} over the depth.

Listing 3.7 Initial Condition with Geothermal Gradient

```
...
#INITIAL_CONDITION
 $PCS_TYPE
  HEAT_TRANSPORT_BHE
 $PRIMARY_VARIABLE
  TEMPERATURE_SOIL
 $GEO_TYPE
  DOMAIN
 $DIS_TYPE
  GRADIENT -120 13.32 0.016
...
```

3.7 Boundary Conditions for the BHE

In Sect. 3.5, the different types of BHE boundary conditions have already been discussed in detail. Besides these configurations, the user still needs to define in the BC file, where the boundary condition should be applied. The following text box shows an example. Here two locations have been specified. The first one was defined on the starting node of the BHE, namely on POINT4. At this location, the inflow temperature was imposed according to curve #1 defined in the RFD file (see Sect. 5.2 for an example). The second location is on POINT9, which is at the bottom of the BHE. This second location is necessary, because OGS will internally read how high the temperature is on the inflow pipe and impose this value on the outflow pipe. Therefore, the value imposed on POINT9 will not have any effect on the simulation result.

Listing 3.8 Boundary condition configuration in the BC file

```
...
#BOUNDARY_CONDITION
 $PCS_TYPE
  HEAT_TRANSPORT_BHE
 $PRIMARY_VARIABLE
  TEMPERATURE_IN_1
 $GEO_TYPE
  POINT POINT4
 $DIS_TYPE
  CONSTANT 1.0
 $TIM_TYPE
  CURVE 1

#BOUNDARY_CONDITION
 $PCS_TYPE
  HEAT_TRANSPORT_BHE
 $PRIMARY_VARIABLE
  TEMPERATURE_OUT_1
 $GEO_TYPE
  POINT POINT9
 $DIS_TYPE
  CONSTANT 5.0
...
```

3.8 Output of Temperatures

In the OUT file, it is configured which of the simulated temperature values are going to be recorded by OGS. As shown in the following example, two different output records are specified, each starting with the key word #OUTPUT. In the first one, the soil temperature over the entire domain is printed out in the PVD format. In the second one, the inlet, outlet temperature of the pipe, the two grout zones surrounding them, and also the soil temperature along the BHE is plotted in the TECPLOT format. Under the key word TIM_TYPE, the specification "STEPS 10" means that the simulation result will be printed once in every ten time steps. Both the PVD format and the TECPLOT format output files can be read by a text editor.

Listing 3.9 The Output Configuration

```
#OUTPUT
  $PCS_TYPE
    HEAT_TRANSPORT_BHE
  $NOD_VALUES
    TEMPERATURE_SOIL
  $GEO_TYPE
    DOMAIN
  $DAT_TYPE
    PVD
  $TIM_TYPE
    STEPS 10
#OUTPUT
  $PCS_TYPE
    HEAT_TRANSPORT_BHE
  $NOD_VALUES
    TEMPERATURE_IN_1_BHE_1
    TEMPERATURE_OUT_1_BHE_1
    TEMPERATURE_G_1_BHE_1
    TEMPERATURE_G_2_BHE_1
    TEMPERATURE_SOIL
  $GEO_TYPE
    POLYLINE BHE_1
  $DAT_TYPE
    TECPLOT
  $TIM_TYPE
    STEPS 10
#STOP
```

3.9 Running the OGS Model

There are several ways to start the simulation. In general, the OGS simulator can be started by calling the executable file ogs.exe. The easiest approach would be to run the simulation in the same folder where the input files are located. After copying the ogs.exe file into the project folder, one can double-click on the executable, then the following windows will appear on the screen (cf. Fig. 3.7). Within this window, one can enter the project name without the dot and any extensions. As the input files are

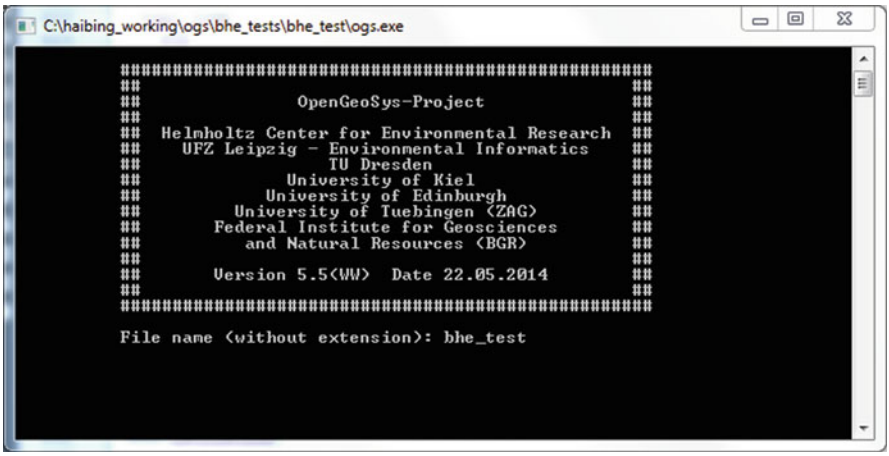

Fig. 3.7 Starting the simulation by calling the executable ogs.exe

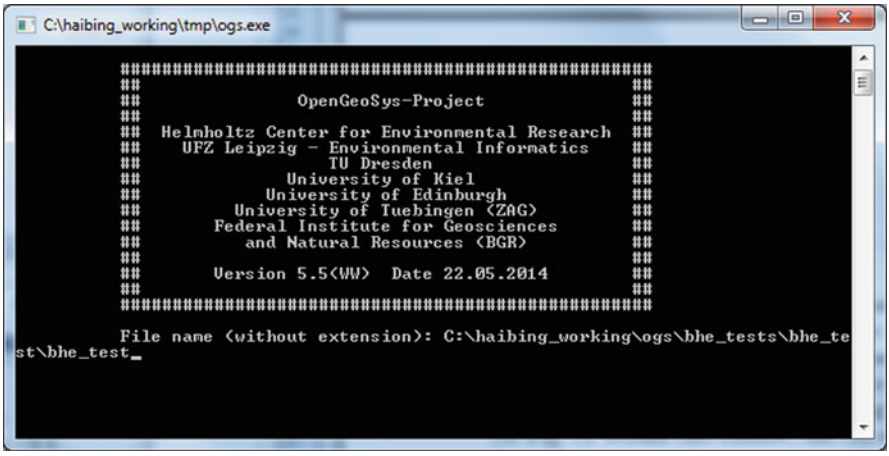

Fig. 3.8 Starting the simulation by calling the executable ogs.exe

name as "bhe_test.∗", entering "bhe_test" will be sufficient. After hitting the Enter key, the simulation will start.

An alternative approach is to have the executable placed at a different location, but supply the executable with the path to the project. As illustrated in Fig. 3.8, now ogs.exe is located under "C:\haibing\working\tmp". After launching ogs.exe, one can enter the project path "C:\haibing_working\ogs\ bhe_tests\bhe_test" to start the simulation. A easier way would be, to drag and drop one of the input files into the OGS command line prompt, and delete the extensions. As the OGS is designed to run on multiple platforms, it can not read in folder or file names with space in

it. Please make sure that the path of the input files does not contain any space or special characters, otherwise OGS will not be able to find the right location.

While running the simulation, there is quiet a lot of logging information being printed on the screen. It includes which time step the simulation is in, how many nonlinear and linear iterations have been conducted, and how big is the numerical residual when solving the linear system. Such information is very helpful to the modeller, therefore it is recommended to save them in a log file. To do this, one could create an empty batch file, eg. named as "run_ogs.bat". Within it, just type in the following content.

Listing 3.10 The content of the batch file

```
ogs.exe bhe_test > result.txt
```

Here the symbol ">" will pipeline the screen output to the file "result.txt". By using this method, the user can open this text file and check the modelling progress while the simulation is still running.

3.10 Visualization of Temperature Evolution

As defined in the OUT file, there are two records in the output configuration, one for the soil temperatures, and the other for the inflow, outflow and grout temperatures on the BHEs (see the introduction in Sect. 3.8).

3.10.1 Visualization of Soil Temperatures

For the soil temperatures, they are recorded in the VTK format, and can be directly visualized by the software Paraview. As shown in Fig. 3.9, the result files are name as "bhe_test_HEAT_TRANSPORT_BHE*.*". The first part of the file name is the same as all the input files, while the second part is composed of the process that was simulated. For each of the *.vtu files, there is a number appending the file name, it reflects which time step this file belongs to. When visualizing the soil temperatures, one could directly load the *.pvd file, making paraview to read in all the printed result. Alternatively, one can also load a single *.vtu file, which only contains the soil temperature distribution at this time step.

Figure 3.10 demonstrates how the soil temperature will be influence by the BHE operation. In this example, the sandbox experiment from Beier et al. (2011) was reproduced (see Sect. 5.2 for more details). Since heat is injected through the U-tubes, the temperature at the center of the sandbox will gradually increase along time. This is reflected by red color at the center of the domain (Fig. 3.10).

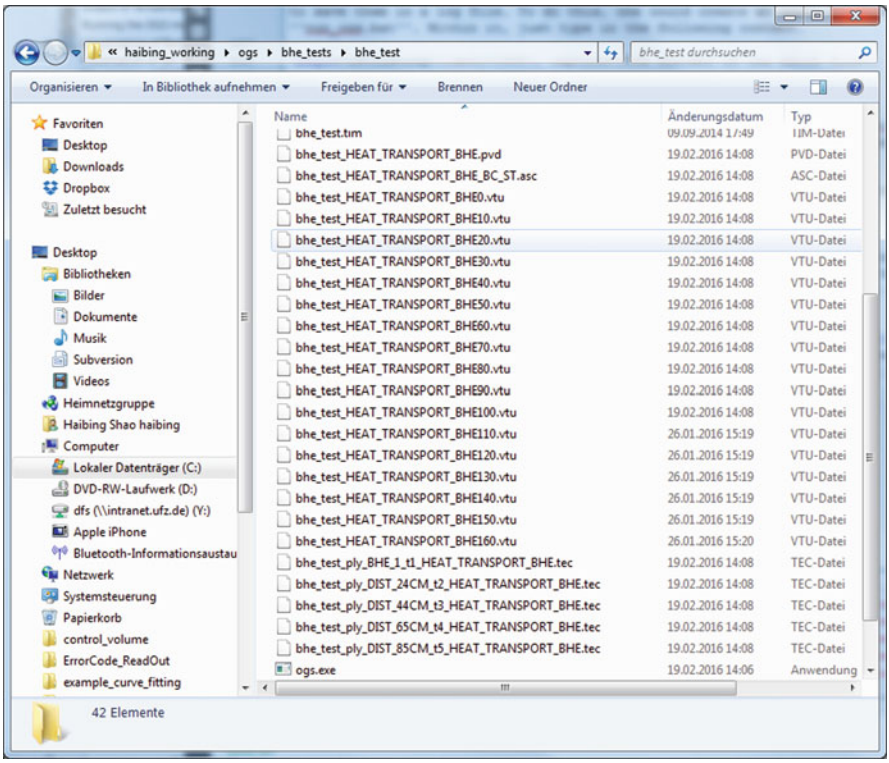

Fig. 3.9 Result files by a simulated OGS project

3.10.2 Visualization of BHE Temperatures

Different from the soil part, the information regarding temperatures inside the borehole heat exchanger is typically printed in the Tecplot file format. Figure 3.11 shows such an example. Here there are altogether six columns listed. From the left to the right, it is the distance from the top of the BHE, temperatures in the inflow and outflow pipeline, temperatures on the two grout zones, and finally BHE wall temperature. The order of the columns is actually defined in the *.out file. Notice that the pipeline temperature values at the bottom of the BHE, specifically on line #24 and #46, are kept the same. One can also import the data into a spreadsheet or plotting software, then the temperature distribution on each BHE can be visualized in a vertical profile.

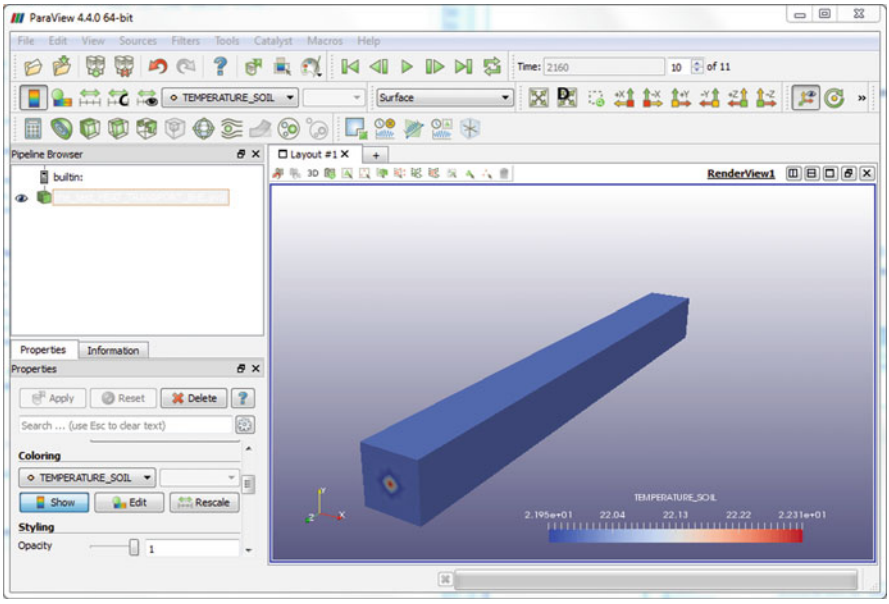

Fig. 3.10 Visualization effect of the simulated soil temperature distribution by the software Paraview

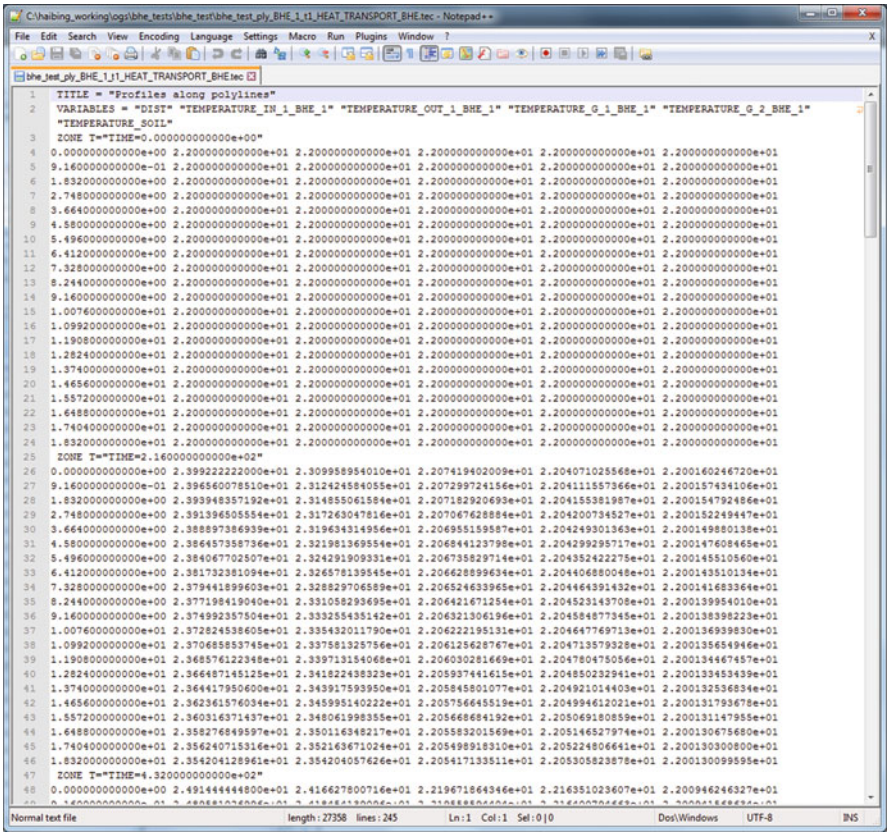

Fig. 3.11 Simulated temperature values printed in the Tecplot file format

Chapter 4
BHE Meshing Tool

In general, there are various approaches to create mesh files. One could try to create the line elements representing BHEs by hand. However, such practice is quiet cumbersome and also very prone to mistakes. To alleviate the user from this burden, a simple meshing tool has been provided. It can be downloaded from the OGS website.

https://docs.opengeosys.org/books/shallow-geothermal-systems

In the provided package, a binary executable has been built for the Windows platform. For users of other platforms, they need to build the meshing tool from the provided source codes.

This meshing tool is capable of creating a 3D prism mesh of the subsurface with arbitrary number of horizontal layers in different thickness, along with different material groups and arbitrary number of vertical BHEs. To use the BHE meshing tool, one also need the software *GMSH*, which is an open-source finite element mesh generator. Software download and tutorials of *GMSH* can be found on its official website (www.gmsh.info). It is necessary to place both binaries files, i.e. the *bhe_meshing_tool.exe* and the *gmsh.exe* in the same working folder.

The work flow is organized in the following order:

(1) Read in the input file.
(2) Create a GMSH geometry file according to specifications defined in the input file.
(3) Call the GMSH to create the 2D surface mesh.
(4) Import the mesh created in step (3).
(5) Extrude the surface mesh according to layer specifications made in the input file.
(6) Generate BHE elements according to specifications made in the input file.
(7) Write the corresponding mesh file into OGS format.
(8) Write the corresponding geometry file into OGS format.

H. Shao et al., *Geoenergy Modeling II*, SpringerBriefs in Energy,
DOI 10.1007/978-3-319-45057-5_4

4.1 Requirement on the Mesh

As mentioned in Diersch et al. (2011b), when the BHE is represented by 1D elements, the amount of heat flux between BHE and the surrounding soil is heavily influenced by the size of mesh elements in the vicinity of the BHE node. To guarantee the accuracy of simulation result, Diersch et al. (2011b) proposed a procedure to determine the optimal nodal distance, that is influenced by the number of nodes surrounding the BHE center node, as well as the borehole diameter. The optimal distance Δ can be obtained by

$$\Delta = ar_b,\ a = e^{\frac{2\pi}{\vartheta}}, \vartheta = n\, tan\frac{\pi}{n}, \tag{4.1}$$

with r_b denotes the borehole radius, and n refers to the number of surrounding nodes. Δ is increasing along with the number n. When designing the mesh with the provided meshing tool, the above criteria has already been considered to ensure the correct heat flux over the borehole wall, which will influence all inlet, outlet and grout temperatures on the BHE nodes. Deviation from Eq. (4.1) will lead to inaccurate solutions. The meshing tool always operates with a number of $n = 6$ nodes. If a different setup is required, the user may want to modify the source code of this meshing tool, which is also provided.

4.2 Input File for the Meshing Tool

To run the meshing tool, one can type the following command.

Listing 4.1 Run the meshing tool

```
>bhe_meshing_tool.exe inputfile
```

Here the *inputfile* is an ASCII file containing all configurations for generating the complete 3D mesh. If the user wishes a 2D mesh output, one can type

Listing 4.2 Run the meshing tool to generate 2D mesh

```
>bhe_meshing_tool.exe inputfile -2D
```

to generate a surface 2D mesh only. This is useful for the inspection of the surface mesh before it will be extruded. All information required to generate a complete mesh including BHEs have to be supplied in the input file. An example is given here and the key words and parameters are explained.

Listing 4.3 Input file: example.inp

```
WIDTH 100
LENGTH 200
DEPTH 90
BOX 50 100 50
// BOX -1 -1 -1
ELEM_SIZE 5 20
LAYER 0 10 1
LAYER 1 20 2
LAYER 2 10 4
BHE 0 -10 100 0 -50 0.063
BHE 1 10 100 0 -30 0.063
```

- `WIDTH`: Domain width in the x-direction. Note that the model is centred in the x-direction. This means, the domain here would extend from −50 to 50 in the x direction.
- `LENGTH`: Domain length in the y-direction. Note that the origin is at the front boundary. In the example above, the domain would extend from y=0..200
- `DEPTH`: Domain thickness in the negative z-direction. Note that the surface is always at z=0. Therefore in the example above, the domain would extend from z=0..−90. This parameter only affects the creation of the geometry file. The mesh will be extruded according to the definition of layers (see the LAYER keyword below).
- `BOX`: Here, a refinement box can be defined. Parameters are
  y-coordinate of the box front
  length of the box
  width of the box
  In the example above, the box would extend from x=−25..25 and y=50..150. If the model shall not contain a refinement box, the values have to be replaced by −1.
- `ELEM_SIZE`: This defines the element size at the boundary of the refinement box and the outer boundaries. If no refinement box is employed, the first value will be overrun.
- `LAYER`: Specification of each layer with following parameters:
  material group index value
  number of elements in this layer
  thickness of each element in this layer
  The thickness of layer is then dependent on the number of elements, as well as the thickness of each element. Please make sure that the definition of domain depth, layers and vertical extent of BHEs match with each other.
- `BHE`: Here, the BHEs are defined with the following parameters:
  Number of BHE (This number is only referring to the total number of BHEs, NOT the corresponding material groups. The material groups will be generated and linked with BHE automatically.)
  x-coordinate of BHE center
  y-coordinate of BHE center
  z-coordinate of BHE top end
  z-coordinate of BHE bottom end

The user has to make sure, that layers boundaries are located properly at the BHE top and bottom ends. The algorithm in the meshing tool will automatically pick up the nearest mesh nodes in the z-direction, and generate BHE elements with these mesh nodes.

4.3 Output

After execution of the meshing tool, the following files will be written in the working folder.

- *example.bhe.msh*: This is the OGS mesh file. In order to use it for running a simulation, one would have to rename it by deleting the extension "*.bhe*" from the file name. The content of this mesh file is listed in the following text box, and the visualized effect of this mesh is illustrated in Figs. 4.1 and 4.2.

Listing 4.4 example.bhe.msh

```
#FEM_MSH
$PCS_TYPE
NO_PCS
$NODES
50512
0 -50 0 0
1 50 0 0
2 50 200 0
3 -50 200 0
[..]
50510 -4.9577 100.738 -90
50511 4.96093 100.753 -90
$ELEMENTS
97330
0 0 pris 1092 122 503 2324 1354 1735
1 0 pris 1091 504 121 2323 1736 1353
2 0 pris 1178 387 233 2410 1619 1465
[..]
24318 0 pris 11502 11834 11973 12734 13066 13205
24319 0 pris 11503 11971 11832 12735 13203 13064
24320 1 pris 13412 12442 12823 14644 13674 14055
24321 1 pris 13411 12824 12441 14643 14056 13673
[..]
72958 1 pris 36142 36474 36613 37374 37706 37845
72959 1 pris 36143 36611 36472 37375 37843 37704
72960 2 pris 38052 37082 37463 39284 38314 38695
72961 2 pris 38051 37464 37081 39283 38696 38313
72962 2 pris 38138 37347 37193 39370 38579 38425
[..]
97278 2 pris 48462 48794 48933 49694 50026 50165
97279 2 pris 48463 48931 48792 49695 50163 50024
97280 3 line 8 1240 97281 3 line 1240 2472
[..]
97308 3 line 34504 35736
97309 3 line 35736 36968
97310 4 line 15 1247
97311 4 line 1247 2479
[..]
97329 4 line 23423 24655
#STOP
```

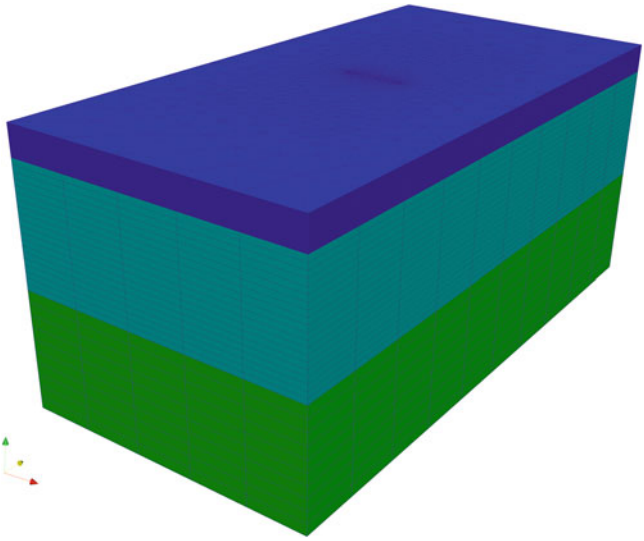

Fig. 4.1 3D mesh

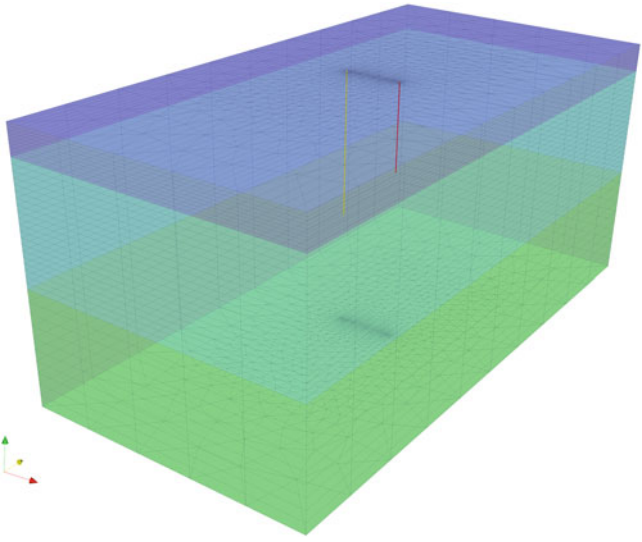

Fig. 4.2 3D mesh, line elements inside

- *example.geo*: This is the geometry input file for GMSH.
- *example.gli*: This is the OGS geometry file (illustrated in Fig. 4.3). The six surfaces of the cube are named as `top, bottom, left, right, inflow, outflow`. Important definitions for the BHEs are the top and bottom points as well as the BHE polylines, which are named in a systematic manner.

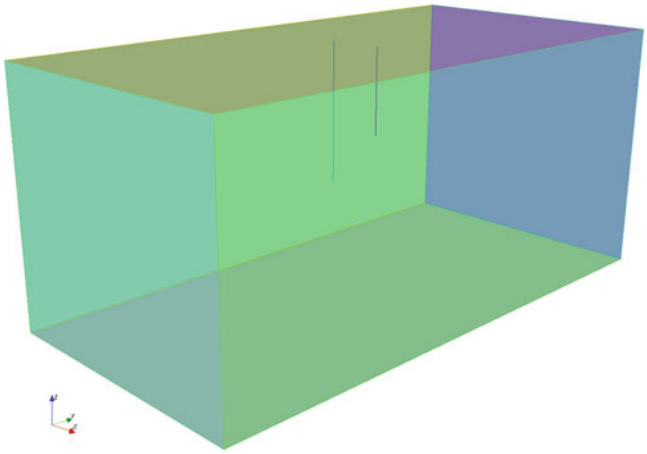

Fig. 4.3 Geometry

Listing 4.5 example.gli

```
#POINTS
0 -50 0 0
1 50 0 0
[..]
8 -10 100 0 $NAME BHE0_top
9 -10 100 -50 $NAME BHE0_bottom
10 10 100 0 $NAME BHE1_top
11 10 100 -30 $NAME BHE1_bottom
[..]
#POLYLINE
$NAME
ply_BHE0
$POINTS
8
9
#POLYLINE
$NAME
ply_BHE1
$POINTS
10
11
[..]
#STOP
```

- *example.msh*: This is the 2D surface mesh generated by GMSH (illustrated in Fig. 4.4). Please notice that this 2D mesh is only generated intermediately and it is NOT for OGS model simulation. For the OGS input, the 3D mesh file *example.bhe.msh* should be used.

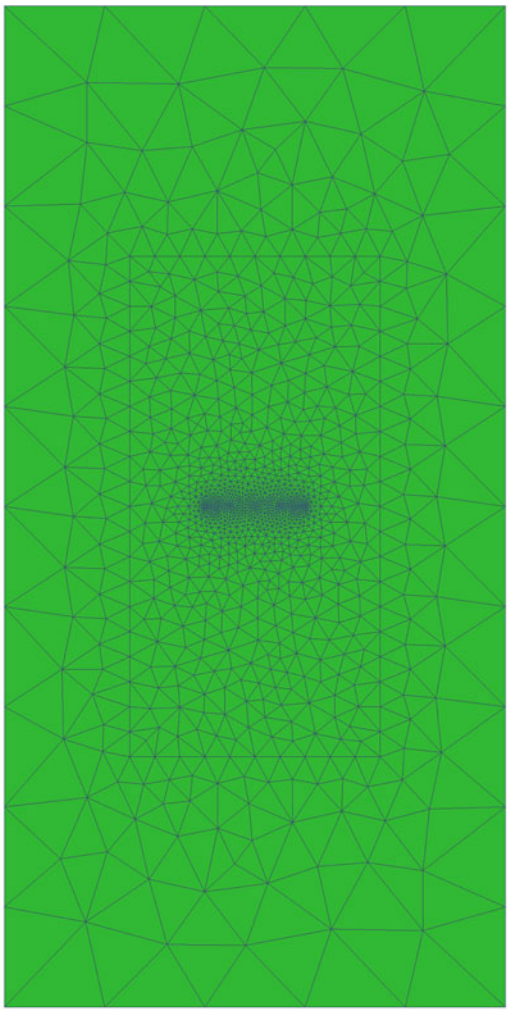

Fig. 4.4 Surface mesh

Chapter 5
Benchmarks

In order to verify both the heat transport process that is induced by the operation of BHEs, two benchmark comparisons have been carried out. In the first case, the result from analytical Infinite Line Source Model has been used as a standard (Sect. 5.1). In the second case, the numerically simulated outflow temperatures have been compared to observations from an indoor sandbox experiment (Sect. 5.2).

5.1 Borehole Heat Exchangers: Comparison to Line Source Model

Here in this benchmark, the soil temperature evolution induced by a BHE is obtained from three different configurations. They are:

- Using the *infinite line source (ILS)* analytical solution, assuming heat is evenly extracted over the length of a BHE.
- By simulating the HEAT_TRANSPORT process using OpenGeoSys, also assuming heat is evenly extracted by the BHE.
- By simulating the newly developed HEAT_TRANSPORT_BHE process in OpenGeoSys. Although the same thermal load is imposed on the BHE, this new process allows the dynamic development of pipeline and grout temperatures as well.

All three configurations have been established with the same geometry, initial conditions, and material parameters etc., which are listed in Table 5.1. It is known that the analytical line source model will produce inaccurate results of soil temperature in the immediate vicinity of the BHE. Nevertheless, the results should converge at a couple of meters away from the BHE. The result comparison will be presented in Sect. 5.1.4.

H. Shao et al., *Geoenergy Modeling II*, SpringerBriefs in Energy,
DOI 10.1007/978-3-319-45057-5_5

Table 5.1 Parameters used in the line source model comparison

Parameter	Symbol	Value	Unit
Specific thermal load on the BHE	q_b	-5.68	W m^{-1}
Length of the BHE	L_{BHE}	46	m
Thermal load on the BHE	Q	-261.68	W
Soil thermal conductivity	λ_{soil}	1.34	W m^{-1} K^{-1}
Heat capacity of soil	$(\rho c_p)_{soil}$	2×10^6	J m^{-3} K^{-1}
BHE type		$1U$	
Diameter of the BHE	D_{BHE}	15	cm
Diameter of the pipeline	d_{pipe}	3.98	cm
Wall thickness of the pipeline	b_{pipe}	0.36	cm
Distance between the pipelines	w	6.3	cm
Thermal conductivity of pipeline wall	λ_{pipe}	0.39	W m^{-1} K^{-1}
Thermal conductivity of the grout	λ_{grout}	0.73	W m^{-1} K^{-1}
Heat capacity of the grout	$(\rho c_p)_{grout}$	3.8×10^6	J m^{-3} K^{-1}
Thermal conductivity of the refrigerant	$\lambda_{refrigerant}$	0.477	W m^{-1} K^{-1}
Heat capacity of the refrigerant	$(\rho c_p)_{refrigerant}$	$3.838 \cdot 10^6$	J m^{-3} K^{-1}
Viscosity of the refrigerant	$\mu_{refrigerant}$	$3.04 \cdot 10^{-3}$	kg m^{-1} s^{-1}
Flow rate of the refrigerant	$Q_{refrigerant}$	15.087	m^3 d^{-1}

5.1.1 ILS Analytical Solution

When using the infinite line source (ILS) solution (Stauffer et al. 2014), soil temperatures are expressed in difference values in comparison to the undisturbed initial temperature T_0 at a radial distance r_b. And this difference is given by

$$T - T_0 = \frac{q_b}{4\pi\lambda} E_1\left(\frac{r_b^2}{4\alpha t}\right) \tag{5.1}$$

with q_b referring to the heat flow rate per length of BHE, thermal diffusivity $\alpha = \frac{\lambda}{\rho c_p}$ and the exponential integral function E_1.

5.1.2 Numerical Line Source Model

In the numerical line source model, a domain has been constructed, with a single BHE located in the middle of it. Here the numerical process HEAT_TRANSPORT has been simulated. A constant source term of q_b was imposed on a polyline representing the BHE (cf. Fig. 5.1). Here, a constant heat source (a Neumann-type of boundary condition) of $-5.68\,\mathrm{W/m}$ is applied on the polyline "BHE_1". The following text box shows how the ST file was defined.

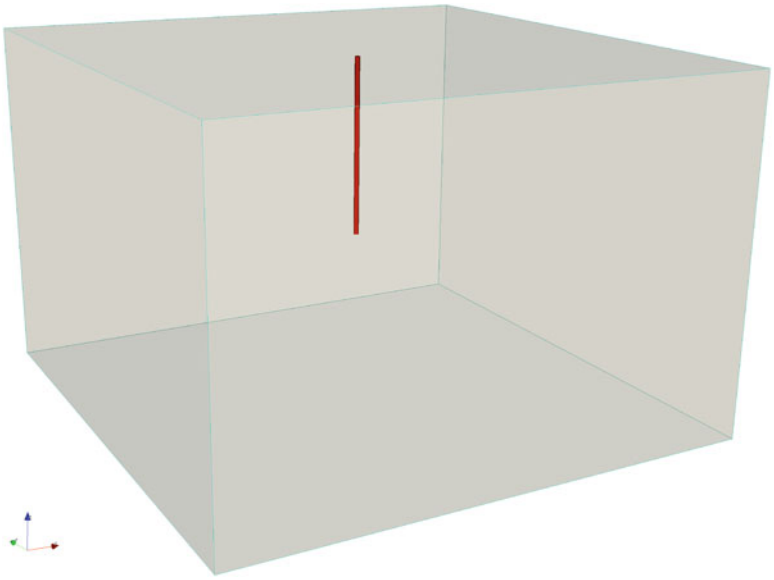

Fig. 5.1 Geometry of the benchmark, with BHE in the centre of the domain, modelled by a line source

Listing 5.1 Source term File (linesource.st)

```
#SOURCE_TERM
 $PCS_TYPE
   HEAT_TRANSPORT
 $PRIMARY_VARIABLE
   TEMPERATURE1
 $GEO_TYPE
   POLYLINE BHE_1
 $DIS_TYPE
   CONSTANT_NEUMANN -5.68
#STOP
```

Other input files of this configuration is summarized in Table 5.2. Interested readers may visit the OpenGeoSys webpage (https://docs.opengeosys.org/books/shallow-geothermal-systems) to download these input files.

5.1.3 Numerical BHE Model

Different from the configuration in Sect. 5.1.2, the numerical BHE model has a different approach to represent the borehole heat exchanger. Here the temperature evolution inside and around the BHE was simulated with a constant power $Q = q_b \cdot L_{BHE}$, and imposed as a boundary condition (cf. Sect. 5.1.4). Such configuration has been reflected in the MMP file (see the text box below). In the MMP file,

Table 5.2 *OGS* input files for the Numerical Line Source model

Object	File	Explanation
GEO	`linesource.gli`	System geometry
MSH	`linesource.msh`	Finite element mesh
PCS	`linesource.pcs`	Process definition
NUM	`linesource.num`	Numerical properties
TIM	`linesource.tim`	Time discretization
IC	`linesource.ic`	Initial conditions
BC	`linesource.bc`	Boundary conditions
ST	`linesource.st`	Source/sink terms
MSP	`linesource.msp`	Solid properties
MMP	`linesource.mmp`	Medium properties
OUT	`linesource.out`	Output configuration

the material group #0 refers to the soil part. Since no groundwater flow process is considered, all values are zero. Material group #1 represents the BHE. Here, all relevant parameters for the BHE model are entered, according to the values given in Table 5.1. What is special here is that, the boundary condition type for the BHEs is set to be "POWER_IN_WATT". This means a fixed thermal load will be imposed on the BHE. The inflow refrigerant temperature will be automatically adjusted to satisfy this thermal load.

Listing 5.2 Medium Properties File (BHE.mmp)

```
#MEDIUM_PROPERTIES
 $GEO_TYPE
  DOMAIN
 $GEOMETRY_DIMENSION
  3
 $GEOMETRY_AREA
  1
 $POROSITY
  1 0.0
 $PERMEABILITY_TENSOR
  ISOTROPIC 0.0
 $HEAT_DISPERSION
  1 0.0 0.0
#MEDIUM_PROPERTIES
 $GEO_TYPE
  POLYLINE BHE_1
 $GEOMETRY_DIMENSION
  1
 $GEOMETRY_AREA
  1
 $BOREHOLE_HEAT_EXCHANGER
  BHE_TYPE
    BHE_TYPE_1U
  BHE_BOUNDARY_TYPE
    POWER_IN_WATT
  BHE_POWER_IN_WATT_VALUE
    -261.28
  BHE_LENGTH
    46
  BHE_DIAMETER
    0.15
```

```
  BHE_REFRIGERANT_FLOW_RATE
    1.746E-04
  BHE_INNER_RADIUS_PIPE
    0.0163
  BHE_OUTER_RADIUS_PIPE
    0.0199
  BHE_PIPE_IN_WALL_THICKNESS
    0.0036
  BHE_PIPE_OUT_WALL_THICKNESS
    0.0036
  BHE_FLUID_TYPE
    0
  BHE_FLUID_LONGITUDIAL_DISPERSION_LENGTH
    0.0
  BHE_GROUT_DENSITY
    2190.0
  BHE_GROUT_POROSITY
    0.0
  BHE_GROUT_HEAT_CAPACITY
    1735.16
  BHE_THERMAL_CONDUCTIVITY_PIPE_WALL
    0.39
  BHE_THERMAL_CONDUCTIVITY_GROUT
    0.73
  BHE_PIPE_DISTANCE
    0.063
#STOP
```

In the BC file, two records have to be made for the inlet temperature at the top of the BHE and the outlet temperature at the bottom of the BHE. These two boundary conditions are required by OGS in order to locate top and bottom nodes of the BHE. Since a power boundary conditions on the BHE has already been defined, the values entered here can be arbitrary, because they will not be considered throughout the simulation.

Listing 5.3 Boundary condition File (BHE.bc)

```
#BOUNDARY_CONDITION
 $PCS_TYPE
   HEAT_TRANSPORT_BHE
 $PRIMARY_VARIABLE
   TEMPERATURE_IN_1
 $GEO_TYPE
   POINT BHE1_TOP
 $DIS_TYPE
   CONSTANT 1.0
#BOUNDARY_CONDITION
 $PCS_TYPE
   HEAT_TRANSPORT_BHE
 $PRIMARY_VARIABLE
   TEMPERATURE_OUT_1
 $GEO_TYPE
   POINT BHE1_BOTTOM
 $DIS_TYPE
   CONSTANT 1.0
#STOP
```

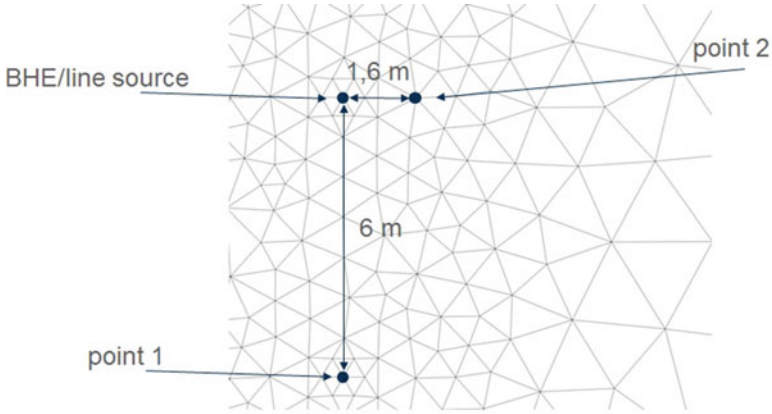

Fig. 5.2 Observation points in line source model

5.1.4 Results

Soil temperatures were observed at two locations, one at a distance of $r_1 = 6.0\,\mathrm{m}$ another at $r_2 = 1.6\,\mathrm{m}$ (c.f. Fig. 5.2). Good agreement has been reached between the analytical line source model solution and the numerical results. The comparison of temperature profiles can be found in Figs. 5.3 and 5.4. From these two figures, it can be concluded that the two numerical model configurations produce correct result regarding the soil temperature evolution. This comparison also suggests that the temperature difference along the BHE length is relatively small. It is safe to assume that the thermal load will be evenly distributed along the entire BHE length, and it will not generate observable changes on the soil temperatures.

5.2 Borehole Heat Exchangers: Comparison to Sandbox Experiment

In this benchmark, the Borehole Heat Exchanger (BHE) feature in the OGS software is validated against experimental results obtained by Beier et al. (2011). In their experiment, a Thermal Response Test (TRT) was performed under controlled conditions on a single U-tube borehole heat exchanger placed inside a sand box. Inlet and outlet fluid temperatures were monitored together with temperatures at the borehole wall and at different locations in the sand box.

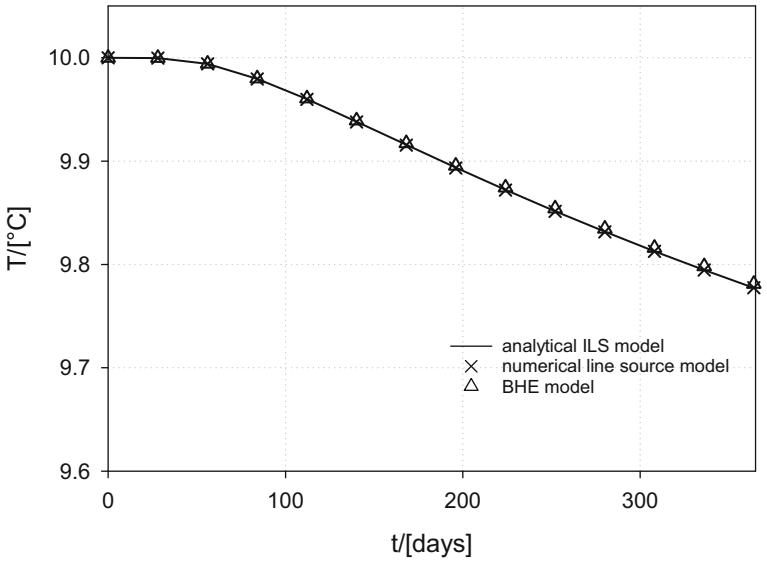

Fig. 5.3 Comparison of soil temperature profile at 6.0 m distance

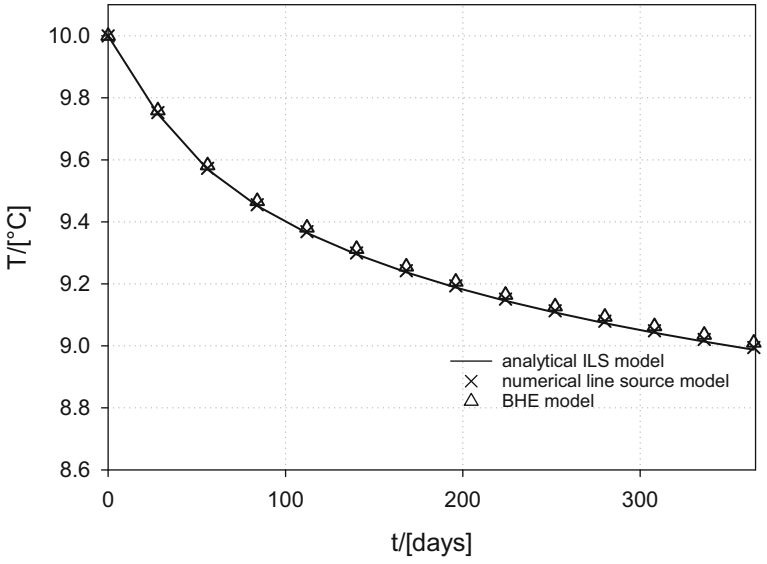

Fig. 5.4 Comparison of soil temperature profile at 1.6 m distance

5.2.1 Model Setup

The model was built according to the experimental configurations. The BHE is represented by line elements which are embedded in a 3D prism mesh representing the sandbox (Fig. 5.5). The length of the box is 18 m with a square cross section of 1.8 m per side. Detailed parameters for the model configuration can be found in Table 5.3.

In Beier's experiment, there was an aluminium pipe acting as the borehole wall. It cannot be represented by the BHE model itself, therefore the borehole diameter was taken as the aluminium pipe's outer diameter of 0.13 m in the numerical model. The grout's thermal conductivity was increased from originally 0.73 W m^{-1} K^{-1} to 0.806 W m^{-1} K^{-1}, in order to include the aluminium pipe's thermal conductivity and its geometry. The BHE is filled with water. Thermal properties and viscosity of water are taken at an average temperature of approx. 36 °C.

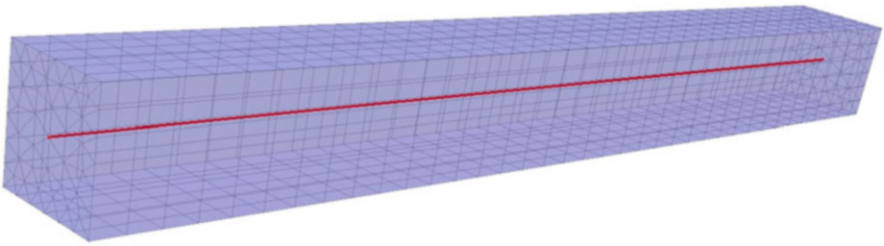

Fig. 5.5 Sandbox model

Table 5.3 Benchmark parameters according to Beier's sandbox experiment (Beier et al. 2011)

Parameter	Symbol	Value	Unit
Soil thermal conductivity	λ_{soil}	2.78	W m^{-1} K^{-1}
Soil heat capacity	$(\rho c_p)_{soil}$	3.2×10^6	J m^{-3} K^{-1}
Diameter of the BHE	D_{BHE}	13	cm
Diameter of the pipeline	d_{pipe}	2.733	cm
Wall thickness of the pipeline	b_{pipe}	0.3035	cm
Distance between pipelines	w	5.3	cm
Pipeline wall thermal conductivity	λ_{pipe}	0.39	W m^{-1} K^{-1}
Grout thermal conductivity	λ_{grout}	0.806	W m^{-1} K^{-1}
Heat capacity of the grout	$(\rho c_p)_{grout}$	3.8×10^6	J m^{-3} K^{-1}

5.2.2 OGS Input Files

The OGS input files used in this benchmark is very similar as those in Sect. 5.1. Here only the unique parts are highlighted.

5.2.2.1 Initial and Boundary Conditions

Initial conditions for fluid inlet/outlet temperatures and wall temperature were directly taken from the measurements at $t = 0$. For the initial soil temperature, the mean value of all sensors placed in the sand was taken. As initial grout temperatures, arithmetic mean between wall and fluid inlet/outlet temperature was taken. Detailed initial temperatures can be found in Table 5.4.

Listing 5.4 Initial Condition File (Beier.ic)

```
#INITIAL_CONDITION
 $PCS_TYPE
   HEAT_TRANSPORT_BHE
 $PRIMARY_VARIABLE
   TEMPERATURE_SOIL
 $GEO_TYPE
   DOMAIN
 $DIS_TYPE
   CONSTANT 22.1
#INITIAL_CONDITION
 $PCS_TYPE
   HEAT_TRANSPORT_BHE
 $PRIMARY_VARIABLE
   TEMPERATURE_SOIL
 $GEO_TYPE
   POLYLINE BHE_1
 $DIS_TYPE
   CONSTANT 21.95
#INITIAL_CONDITION
 $PCS_TYPE
   HEAT_TRANSPORT_BHE
 $PRIMARY_VARIABLE
   TEMPERATURE_IN_1
 $GEO_TYPE
   POLYLINE BHE_1
 $DIS_TYPE
   CONSTANT 22.21
```

Table 5.4 Initial conditions of sandbox model

Parameter	Symbol	Value	Unit
BHE inlet temperature	T_{in}	22.21	°C
BHE outlet temperature	T_{out}	21.98	°C
Grout temperature around inlet pipe	T_{grout1}	22.08	°C
Grout temperature around outlet pipe	T_{grout2}	21.97	°C
Soil temperature	T_{soil}	22.10	°C
BHE wall temperature	T_{wall}	21.95	°C

```
#INITIAL_CONDITION
 $PCS_TYPE
   HEAT_TRANSPORT_BHE
 $PRIMARY_VARIABLE
   TEMPERATURE_OUT_1
 $GEO_TYPE
   POLYLINE BHE_1
 $DIS_TYPE
   CONSTANT 21.98
#INITIAL_CONDITION
 $PCS_TYPE
   HEAT_TRANSPORT_BHE
 $PRIMARY_VARIABLE
   TEMPERATURE_G_1
 $GEO_TYPE
   POLYLINE BHE_1
 $DIS_TYPE
   CONSTANT 22.08
#INITIAL_CONDITION
 $PCS_TYPE
   HEAT_TRANSPORT_BHE
 $PRIMARY_VARIABLE
   TEMPERATURE_G_2
 $GEO_TYPE
   POLYLINE BHE_1
 $DIS_TYPE
   CONSTANT 21.965
#STOP
```

The boundary conditions are imposed on the BHE as time series of measured inlet fluid temperature and flow rate as demonstrated in Fig. 5.6. Note that the BHE top boundary condition is different (cf. MMP file), as the inlet temperature is imposed here as a time series dataset. A constant value `CONSTANT 1.0` is given in the BC file, which will be multiplied with the corresponding value read from `CURVE 1` in the RFD data file.

Listing 5.5 Boundary Condition File (Beier.bc)

```
#BOUNDARY_CONDITION
$PCS_TYPE
HEAT_TRANSPORT_BHE
$PRIMARY_VARIABLE
TEMPERATURE_IN_1
$GEO_TYPE
POINT POINT9
$DIS_TYPE
CONSTANT 1.0
$TIM_TYPE
CURVE 1
#BOUNDARY_CONDITION
$PCS_TYPE
HEAT_TRANSPORT_BHE
$PRIMARY_VARIABLE
TEMPERATURE_OUT_1
$GEO_TYPE
POINT POINT4
$DIS_TYPE
CONSTANT 1.0
#STOP
```

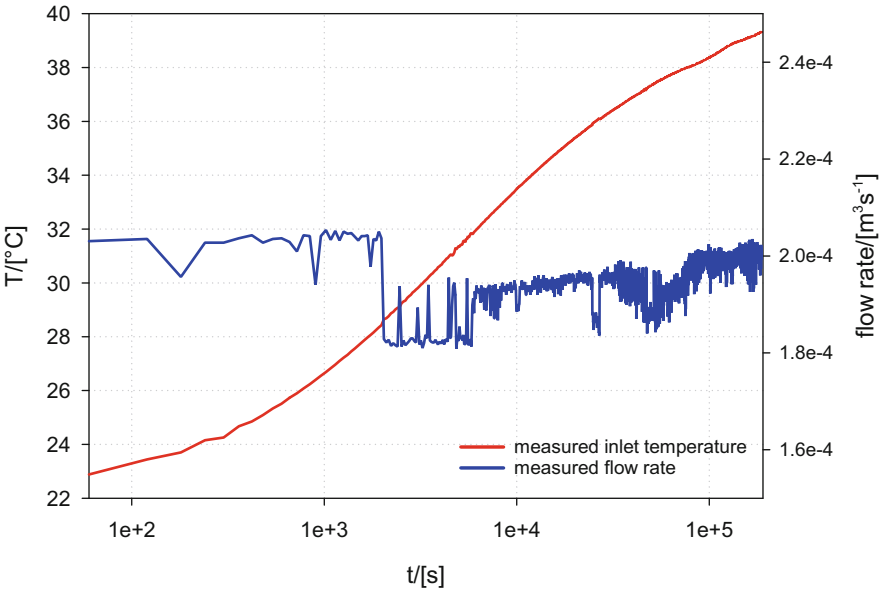

Fig. 5.6 Time series of inlet temperature and flow rate

5.2.2.2 RFD Data File

In this file, time-dependent curves can be defined. In this benchmark, the first curve is the BHE inlet temperature, the second curve is the flow rate.

Listing 5.6 Data File (Beier.rfd)

```
#CURVE
0 22.21111111
60 22.9
120 23.46111111
180 23.72222222
240 24.17222222
300 24.27222222
360 24.68888889
[..]
186180 39.32222222
186240 39.32222222
186300 39.33888889
186360 39.32222222
#CURVE
0 0
60 0.000203129
120 0.000203576
180 0.000195764
[..]
186240 0.000200406
186300 0.000199655
186360 0.000201159
#STOP
```

5.2.2.3 Medium Properties

Please note, that the BHE_BOUNDARY_TYPE is different here as the inlet temperature is imposed. Therefore, the "BHE_BOUNDARY_TYPE" is set to "FIXED_INFLOW_TEMP_CURVE". An index value is also given under the key word "BHE_FLOW_RATE_CURVE_IDX". Other BHE configurations follow those provided by Beier et al. (2011).

Listing 5.7 Medium Properties File (Beier.mmp)

```
#MEDIUM_PROPERTIES
$GEO_TYPE
DOMAIN
$GEOMETRY_DIMENSION
3
$GEOMETRY_AREA
1
$POROSITY
1 0.0
$PERMEABILITY_TENSOR
ISOTROPIC 0.0
$HEAT_DISPERSION
1 0.0 0.0
#MEDIUM_PROPERTIES
$GEO_TYPE
POLYLINE BHE_1
$GEOMETRY_DIMENSION
1
$GEOMETRY_AREA
1
$BOREHOLE_HEAT_EXCHANGER
BHE_TYPE
 BHE_TYPE_1U
BHE_BOUNDARY_TYPE
 FIXED_INFLOW_TEMP_CURVE
BHE_FLOW_RATE_CURVE_IDX
 2
BHE_LENGTH
 18.0
BHE_DIAMETER
 0.13
BHE_REFRIGERANT_FLOW_RATE
 2.0e-4
BHE_INNER_RADIUS_PIPE
 0.013665
BHE_OUTER_RADIUS_PIPE
 0.0167
BHE_PIPE_IN_WALL_THICKNESS
 0.003035
BHE_PIPE_OUT_WALL_THICKNESS
 0.003035
BHE_FLUID_TYPE
 0
BHE_FLUID_LONGITUDIAL_DISPERSION_LENGTH
 0.0
BHE_GROUT_DENSITY
 2190.0
BHE_GROUT_POROSITY
 0.0
BHE_GROUT_HEAT_CAPACITY
 1735.160
BHE_THERMAL_CONDUCTIVITY_PIPE_WALL
```

```
 0.39
BHE_THERMAL_CONDUCTIVITY_GROUT
 0.806
BHE_PIPE_DISTANCE
 0.053
#STOP
```

5.2.3 *Results*

The outlet temperature (Fig. 5.7) as well as the borehole wall temperature, soil temperatures at 24 cm and 44 cm distance to the wall (Fig. 5.8) were compared to the experimental results. It can be observed that a good match has been achieved between experimental and simulation results. The largest relative error is about 2.5 % on the wall temperature. Considering the error of measuring temperatures, flow rate and thermal conductivity values are in the same range, it can be concluded that the numerical model is fully validated.

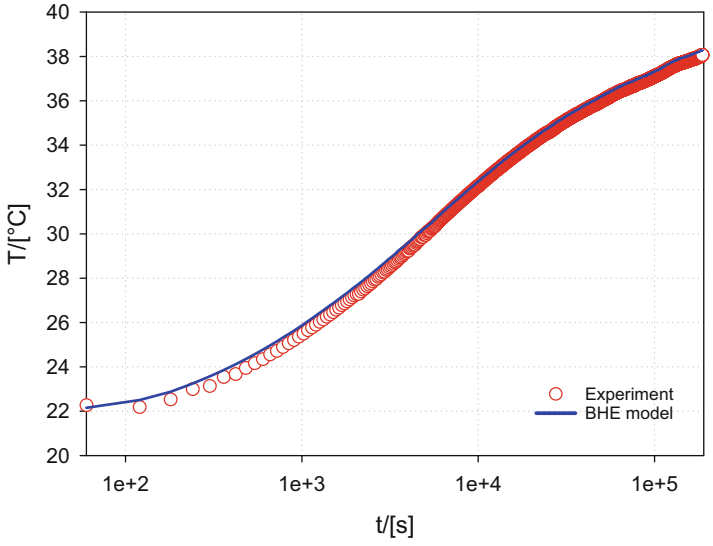

Fig. 5.7 Comparison of simulated and measured outlet temperature profile in the sandbox experiment

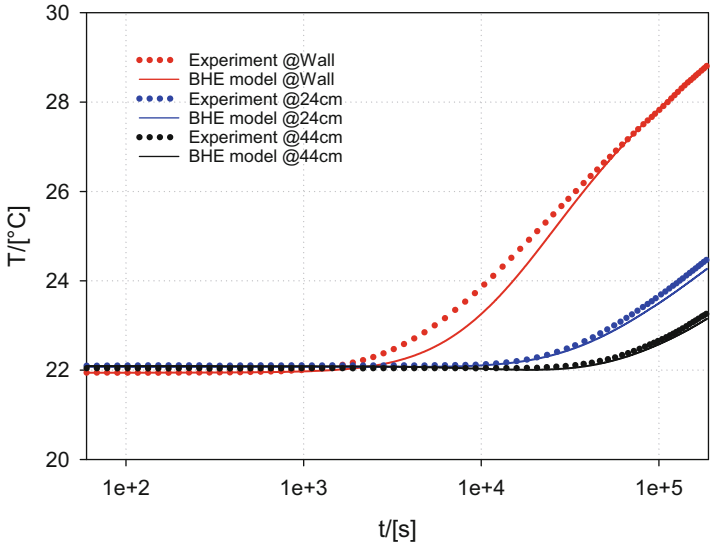

Fig. 5.8 Comparison of modelled and measured wall and soil temperatures

Chapter 6
Case Study: A GSHP System in the Leipzig Area

6.1 The Leipzig-Area Model

In this case study, a simulation was set up and performed in order to predict the long-term performance of the BHE system over a period of 30 years. For that purpose, a simulation scenario was developed including

- a one-family house with its typical heating demand
- a load curve based on this heating demand
- heat pump performance characteristics
- site-specific subsurface conditions in the Leipzig area
- BHE design according to German guideline VDI 4640 (cf. The Association of German Engineers (Verein Deutscher Ingenieure) 2015) considering the load and site-specific parameterization
- local ground surface temperature data, geothermal gradient and heat flux due to measurements in the region of Leipzig.

6.1.1 Scenario

The one-family house has an area of 150 m^2 and is equipped with a floor heating with a design temperature of 35 °C. The specific annual heating demand is 95 kWh $m^{-2}a^{-1}$. This gives a total energy demand of 14,250 kWh, which is distributed over the year with monthly mean values plotted in Fig. 6.1. For the heat pump, a linear relationship between COP and outlet temperature is assumed to be following Eq. (3.2), with coefficient a = 0.083 and b = 3.925 (Glen Dimplex Deutschland GmbH).

H. Shao et al., *Geoenergy Modeling II*, SpringerBriefs in Energy,
DOI 10.1007/978-3-319-45057-5_6

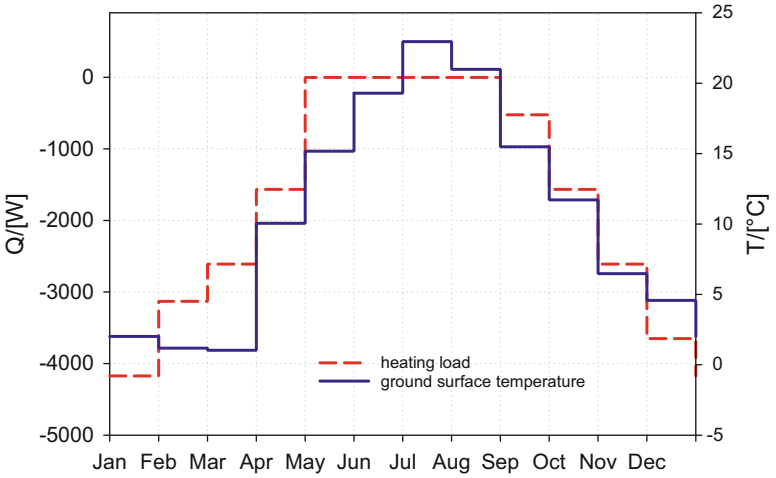

Fig. 6.1 Ground surface temperature and heat pump load

6.1.2 BHE Design

For the design of the system, a *seasonal coefficient of performance (SCOP)* of 4.0 was assumed, and 2100 h of annual operation was adopted. Following VDI guideline (The Association of German Engineers (Verein Deutscher Ingenieure) 2015), this results in a BHE design load of 5.09 kW:

$$P_{BHE} = \left(1 - \frac{1}{SCOP}\right) \frac{E_{annual}}{h_{operation}}. \tag{6.1}$$

With specific heat extraction rates of each layer, which were computed according to Panteleit and Reichling (cf. Panteleit and Reichling 2006), the total length of the BHE evaluates to 93 m. The circulating fluid in the BHE is water with 30 % of ethylene-glycol as anti-freezer. The flow rate is chosen to maintain a turbulent flow in order to have sufficient heat transfer between the fluid and the pipe walls. Details on the BHE parameters are given in Table 6.1.

6.1.3 Model Domain

The size of the computational domain was chosen to be sufficiently large, so that the model boundaries remain undisturbed. It extends 300 m in width, 600 m long and 150 m deep. The model was meshed using the BHE meshing tool (Chap. 4). The input file for the meshing tool is listed below. The resulting mesh is shown in Fig. 6.2.

Table 6.1 Model parameters applied in the Leipzig-area case study

Parameter	Symbol	Value	Unit
Diameter of the borehole	D_{BHE}	0.126	m
Inner diameter of the pipe	d_p	0.02733	m
Thickness of the pipe wall	b_p	0.003035	m
Distance between the pipes	w	0.053	m
Thermal conductivity of the pipe wall	λ_p	0.39	$\mathrm{W\,m^{-1}\,K^{-1}}$
Thermal conductivity of the grout	λ_g	0.73	$\mathrm{W\,m^{-1}\,K^{-1}}$
Heat capacity of the grout	$\rho_g c_g$	3.8×10^6	$\mathrm{J\,m^{-3}\,K^{-1}}$
Refrigerant flow rate	Q_r	2.7×10^{-4}	$\mathrm{m^3\,s^{-1}}$

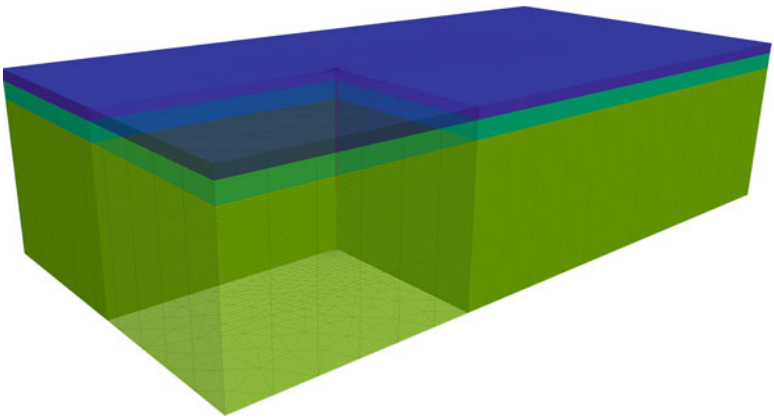

Fig. 6.2 Mesh of Leipzig-area model

Listing 6.1 Input file for meshing tool: taucha.inp

```
WIDTH 300
LENGTH 600
DEPTH 150
BOX 100 300 120
ELEM_SIZE 10 35
LAYER 0 18 0.5
LAYER 1 14 1
LAYER 2 37 2
LAYER 2 1  1
LAYER 2 26 2
BHE 0 0 200 -5 -98 0.063
```

6.1.4 Initial and Boundary Conditions

As an initial condition on the subsurface, the temperature distribution due to the geothermal gradient of 0.016 K $\mathrm{m^{-1}}$ with a temperature of 13 °C at a depth of 100 m

in the region of Leipzig was applied (cf. Richter et al. 2015). The geothermal heat flux, which is applied as a Neumann boundary condition at the bottom surface, is computed according to

$$q_{geo} = \lambda_{eff} \frac{dT}{dZ} \tag{6.2}$$

with

$$\lambda_{eff} = \frac{1}{\sum_{i=1}^{n_{layers}} \frac{\delta_i}{\lambda_i}} \tag{6.3}$$

and evaluates to 0.0527 W m^{-2}. Furthermore, monthly mean values of the ground surface temperature (cf. Leipzig Institute for Meteorology - LIM, Faculty of Physics and Earth Sciences, University Leipzig 2016, Fig. 6.1) are applied as a Dirichlet boundary condition at the top surface.

6.1.5 Input Files

Similar as demonstrated in Chap. 3, the model information is defined in several input files. Here they are listed explicitly with explanations.

6.1.6 Geometry

In this case study, the model domain is a 150×150×200 m cube. The domain was designed to be large enough so that the thermal plume induced by BHE will never reach the model boundary. The BHE starts from 5 m beneath the surface. Such configuration is intended to avoid numerical instability caused by the surface temperature variation.

Listing 6.2 Geometry File (taucha.gli)

```
#POINTS
0 -150 0 0
1 150 0 0
2 150 600 0
3 -150 600 0
4 -150 0 -150
5 150 0 -150
6 150 600 -150
7 -150 600 -150
8 0 200 -5 $NAME BHE0_top
9 0 200 -98 $NAME BHE0_bottom
#POLYLINE
$NAME
ply_top
```

```
$POINTS
0
1
2
3
0
#POLYLINE
$NAME
ply_bottom
$POINTS
4
5
6
7
4
[...]
#POLYLINE
$NAME
ply_inflow
$POINTS
0
1
5
4
0
#POLYLINE
$NAME
ply_outflow
$POINTS
3
2
6
7
3
#POLYLINE
$NAME
ply_BHE0
$POINTS
8
9
#SURFACE
$NAME
top
$POLYLINES
ply_top
#SURFACE
$NAME
bottom
$POLYLINES
ply_bottom
#SURFACE
$NAME
left
[...]
#SURFACE
$NAME
inflow
$POLYLINES
ply_inflow
#SURFACE
$NAME
outflow
$POLYLINES
ply_outflow
#STOP
```

6.1.7 Process Definition

Here both GROUNDWATER_FLOW and HEAT_TRANSPORT_SOIL process are included in the model. However, the groundwater flow velocity is adjusted by the head difference at two ends of the model. Such configuration allows the user to explore the influence of groundwater on the heat transport process.

Listing 6.3 Process definition File (taucha.pcs)

```
#PROCESS
 $PCS_TYPE
  GROUNDWATER_FLOW
 $DEACTIVATED_SUBDOMAIN
  1
  4

#PROCESS
 $PCS_TYPE
  HEAT_TRANSPORT_BHE
 $PRIMARY_VARIABLE
  TEMPERATURE_SOIL

#STOP
```

6.1.8 Numerical Properties

The numerical criteria is defined here for the simulation. A tolerance of 1e-14 was specified for the linear solver, and 1e-3 was set for the Picard iterations.

Listing 6.4 Numerics File (taucha.num)

```
#NUMERICS
 $PCS_TYPE
  GROUNDWATER_FLOW
 $LINEAR_SOLVER
  2      5 1.e-014       100            1.0   100     4
 $ELE_GAUSS_POINTS
  3

#NUMERICS
 $PCS_TYPE
  HEAT_TRANSPORT_BHE
 $LINEAR_SOLVER
  2      5 1.e-14        100            1.0   100     4
 $ELE_GAUSS_POINTS
  3
 $NON_LINEAR_SOLVER
  PICARD 1e-3            250          0.0

#STOP
```

6.1.9 Time Discretization

In this case, a uniform time stepping scheme is imposed. Each time step is about 72 h. The simulation will run for 30 years.

Listing 6.5 Time discretization File (taucha.tim)

```
#TIME_STEPPING
 $PCS_TYPE
  GROUNDWATER_FLOW
 $TIME_START
  0
 $TIME_END
  964224000
 $TIME_STEPS
  3720 259200

#TIME_STEPPING
 $PCS_TYPE
  HEAT_TRANSPORT_BHE
 $TIME_START
  0
 $TIME_END
  964224000
 $TIME_STEPS
  3720 259200

#STOP
```

6.1.10 Initial and Boundary Conditions

For the initial condition, a geothermal gradient is specified. All temperatures on the BHE are configured to be the average soil temperature.

Listing 6.6 Initial Condition File (taucha.ic)

```
#INITIAL_CONDITION
 $PCS_TYPE
  GROUNDWATER_FLOW
 $PRIMARY_VARIABLE
  HEAD
 $GEO_TYPE
  DOMAIN
 $DIS_TYPE
  CONSTANT 75.13

#INITIAL_CONDITION
 $PCS_TYPE
  HEAT_TRANSPORT_BHE
 $PRIMARY_VARIABLE
  TEMPERATURE_SOIL
 $GEO_TYPE
  DOMAIN
 $DIS_TYPE
```

```
  GRADIENT -120 13.32 0.016

#INITIAL_CONDITION
 $PCS_TYPE
  HEAT_TRANSPORT_BHE
 $PRIMARY_VARIABLE
  TEMPERATURE_IN_1
 $GEO_TYPE
  POLYLINE ply_BHE0
 $DIS_TYPE
  CONSTANT 12.6

#INITIAL_CONDITION
 $PCS_TYPE
  HEAT_TRANSPORT_BHE
 $PRIMARY_VARIABLE
  TEMPERATURE_OUT_1
 $GEO_TYPE
  POLYLINE ply_BHE0
 $DIS_TYPE
  CONSTANT 12.6

#INITIAL_CONDITION
 $PCS_TYPE
  HEAT_TRANSPORT_BHE
 $PRIMARY_VARIABLE
  TEMPERATURE_G_1
 $GEO_TYPE
  POLYLINE ply_BHE0
 $DIS_TYPE
  CONSTANT 12.6

#INITIAL_CONDITION
 $PCS_TYPE
  HEAT_TRANSPORT_BHE
 $PRIMARY_VARIABLE
  TEMPERATURE_G_2
 $GEO_TYPE
  POLYLINE ply_BHE0
 $DIS_TYPE
  CONSTANT 12.6

#STOP
```

Regarding the boundary condition, a fluctuating surface temperature was specified, which refers to the curve #2 in the RFD file. This curve was generated by connecting annual temperature curve one after the other.

Listing 6.7 Boundary Condition File (taucha.bc)

```

#BOUNDARY_CONDITION
 $PCS_TYPE
  GROUNDWATER_FLOW
 $PRIMARY_VARIABLE
  HEAD
 $GEO_TYPE
  SURFACE inflow
 $DIS_TYPE
  CONSTANT 75.4

#BOUNDARY_CONDITION
 $PCS_TYPE
  GROUNDWATER_FLOW
 $PRIMARY_VARIABLE
  HEAD
```

```
 $GEO_TYPE
  SURFACE outflow
 $DIS_TYPE
  CONSTANT 74.86

#BOUNDARY_CONDITION
 $PCS_TYPE
  HEAT_TRANSPORT_BHE
 $PRIMARY_VARIABLE
  TEMPERATURE_IN_1
 $GEO_TYPE
  POINT BHE0_top
 $DIS_TYPE
  CONSTANT 1.0

#BOUNDARY_CONDITION
 $PCS_TYPE
  HEAT_TRANSPORT_BHE
 $PRIMARY_VARIABLE
  TEMPERATURE_OUT_1
 $GEO_TYPE
  POINT BHE0_bottom
 $DIS_TYPE
  CONSTANT 1.0

#BOUNDARY_CONDITION
 $PCS_TYPE
  HEAT_TRANSPORT_BHE
 $PRIMARY_VARIABLE
  TEMPERATURE_SOIL
 $GEO_TYPE
  SURFACE inflow
 $DIS_TYPE
  GRADIENT -120 13.32 0.016

#BOUNDARY_CONDITION
 $PCS_TYPE
  HEAT_TRANSPORT_BHE
 $PRIMARY_VARIABLE
  TEMPERATURE_SOIL
 $GEO_TYPE
  SURFACE top
 $DIS_TYPE
  CONSTANT 1.0
 $TIM_TYPE
  CURVE 2

#STOP
```

Here for the source term, a fixed heat flux term is specified, representing the heat conducted from the deep earth.

Listing 6.8 Source term File (taucha.st)

```
#SOURCE_TERM
 $PCS_TYPE
  HEAT_TRANSPORT_BHE
 $PRIMARY_VARIABLE
  TEMPERATURE_SOIL
 $GEO_TYPE
  SURFACE bottom
 $DIS_TYPE
  CONSTANT_NEUMANN 0.0527

#STOP
```

6.1.11 Data RFD File

There are four different curves specified in the RFD file. The first one refers to the building thermal load, which will be applied on the heat pump. The second one is the surface temperature variation. The third and fourth curve are the COP curves of the heat pump. The former one is specified for the heating mode and the latter for the cooling applications.

Listing 6.9 Data File (taucha.rfd)

```
; heat pump load
#CURVE
0 0
31103999 0
31104000 -521
33695999 -521
33696000 -1563
36287999 -1563
36288000 -2604
38879999 -2604
38880000 -3646
41471999 -3646
41472000 -4167
44063999 -4167
44064000 -3125
46655999 -3125
46656000 -2604
49247999 -2604
49248000 -1563
51839999 -1563
51840000 0
54431999 0
54432000 0
57023999 0
57024000 0
59615999 0
59616000 0
62207999 0
[...]
933120000 -521
935711999 -521
935712000 -1563
938303999 -1563
938304000 -2604
940895999 -2604
940896000 -3646
943487999 -3646
943488000 -4167
946079999 -4167
946080000 -3125
948671999 -3125
948672000 -2604
951263999 -2604
951264000 -1563
953855999 -1563
953856000 0
956447999 0
956448000 0
959039999 0
959040000 0
961631999 0
961632000 0
964223999 0
964224000 -521
```

```
; surface temperature
#CURVE
0 15.51
2591999 15.51
2592000 11.74
5183999 11.74
5184000 6.50
7775999 6.50
7776000 4.60
10367999 4.60
10368000 2.04
12959999 2.04
12960000 1.21
15551999 1.21
15552000 1.06
18143999 1.06
18144000 10.07
20735999 10.07
20736000 15.19
23327999 15.19
23328000 19.31
25919999 19.31
25920000 22.96
28511999 22.96
28512000 21.00
31103999 21.00
[...]
933120000 15.51
935711999 15.51
935712000 11.74
938303999 11.74
938304000 6.50
940895999 6.50
940896000 4.60
943487999 4.60
943488000 2.04
946079999 2.04
946080000 1.21
948671999 1.21
948672000 1.06
951263999 1.06
951264000 10.07
953855999 10.07
953856000 15.19
956447999 15.19
956448000 19.31
959039999 19.31
959040000 22.96
961631999 22.96
961632000 21.00
964223999 21.00
964224000 15.51

; Curve for COP 35 deg C floor heating
#CURVE
-5.0 3.5
25.0 6.0

; Curve for COP 18 deg C cooling
#CURVE
5.0 8.0
30.0 5.0

#STOP
```

6.1.12 Fluid Properties

Here two fluid properties are defined. The first one is the groundwater, and the second one refers to the refrigerant circulating in the U-tube.

Listing 6.10 Fluid Properties File (taucha.mfp)

```
; properties of groundwater
#FLUID_PROPERTIES
 $FLUID_TYPE
  LIQUID
 $PCS_TYPE
  GROUNDWATER_FLOW
 $DENSITY
  1  999.25
 $VISCOSITY
  1  1.1929E-03
 $SPECIFIC_HEAT_CAPACITY
   1 4085.9
 $HEAT_CONDUCTIVITY
   1 0.59214

; properties of refrigerant, ethylen glycol 30%
#FLUID_PROPERTIES
 $FLUID_TYPE
  REFRIGERANT
 $PCS_TYPE
  HEAT_TRANSPORT_BHE
 $DENSITY
  1  1045.4
 $VISCOSITY
  1  3.8315E-03
 $SPECIFIC_HEAT_CAPACITY
   1 3661.7
 $HEAT_CONDUCTIVITY
   1 0.47222

#STOP
```

6.1.13 Solid Phase Properties

In the MSP file, the thermal conductivity and heat capacity values are defined. Depending on the different type of sediments, these values are also slightly different.

Listing 6.11 Solid Properties File (taucha.msp)

```
; properties of soil
;MG 0 Geschiebemergel
#SOLID_PROPERTIES
 $DENSITY
  1 1000.0
 $THERMAL
  EXPANSION
   1 0.0
```

```
  CAPACITY
   1 2000.0
  CONDUCTIVITY
   1 1.34

;MG 1 Aquifer
 #SOLID_PROPERTIES
 $DENSITY
  1 1000.0
 $THERMAL
  EXPANSION
   1 0.0
  CAPACITY
   1 2500.0
  CONDUCTIVITY
   1 2.40

;MG 2 Stauer
#SOLID_PROPERTIES
 $DENSITY
  1 1000.0
 $THERMAL
  EXPANSION
   1 0.0
  CAPACITY
   1 2150.0
  CONDUCTIVITY
   1 3.85

; dummy properties for BHE
#SOLID_PROPERTIES
 $DENSITY
  1 0.0
 $THERMAL
  EXPANSION
   1 0.0
  CAPACITY
   1 0.0
  CONDUCTIVITY
   1 0.0

#STOP
```

6.1.14 Medium Properties

Here in the medium property file, BHE parameters are defined. Notice that a special boundary condition is assigned to the BHE, which is the building thermal load. The model will automatically calculate the COP value based the simulated outflow temperature. Such feature allows a more realistic modelling of the GSHP system.

Listing 6.12 Medium Properties File (taucha.mmp)

```
;properties of soil
;layer 0
#MEDIUM_PROPERTIES
 $GEO_TYPE
  DOMAIN
```

```
 $GEOMETRY_DIMENSION
  3
 $GEOMETRY_AREA
  1
 $POROSITY
  1 0.0
 $PERMEABILITY_TENSOR
  ISOTROPIC 5.0E-07
 $HEAT_DISPERSION
  1 0.0 0.0

;layer 1
#MEDIUM_PROPERTIES
 $GEO_TYPE
  DOMAIN
 $GEOMETRY_DIMENSION
  3
 $GEOMETRY_AREA
  1
 $POROSITY
  1 0.0
 $PERMEABILITY_TENSOR
  ISOTROPIC 7.2E-04
 $HEAT_DISPERSION
  1 0.0 0.0

;layer 2
#MEDIUM_PROPERTIES
 $GEO_TYPE
  DOMAIN
 $GEOMETRY_DIMENSION
  3
 $GEOMETRY_AREA
  1
 $POROSITY
  1 0.0
 $PERMEABILITY_TENSOR
  ISOTROPIC 5.1E-06
 $HEAT_DISPERSION
  1 0.0 0.0

; properties of BHE 0
#MEDIUM_PROPERTIES
 $GEO_TYPE
   POLYLINE ply_BHE0
 $GEOMETRY_DIMENSION
   1
 $GEOMETRY_AREA
   1
 $BOREHOLE_HEAT_EXCHANGER
  BHE_TYPE
    BHE_TYPE_1U
  BHE_BOUNDARY_TYPE
    BHE_BOUND_BUILDING_POWER_IN_WATT_CURVE_FIXED_FLOW_RATE
  BHE_POWER_IN_WATT_CURVE_IDX
    1
  BHE_HP_HEATING_COP_CURVE_IDX
    3
  BHE_HP_COOLING_COP_CURVE_IDX
    4
  BHE_LENGTH
    93
  BHE_DIAMETER
    0.126
  BHE_REFRIGERANT_FLOW_RATE
    2.7E-04
  BHE_INNER_RADIUS_PIPE
```

```
    0.0137
  BHE_OUTER_RADIUS_PIPE
    0.0167
  BHE_PIPE_IN_WALL_THICKNESS
    0.003
  BHE_PIPE_OUT_WALL_THICKNESS
    0.003
  BHE_FLUID_TYPE
    1
 BHE_FLUID_LONGITUDIAL_DISPERSION_LENGTH
    0.0
  BHE_GROUT_DENSITY
    2190.0
  BHE_GROUT_POROSITY
    0.0
  BHE_GROUT_HEAT_CAPACITY
    1735.16
  BHE_THERMAL_CONDUCTIVITY_PIPE_WALL
    0.39
  BHE_THERMAL_CONDUCTIVITY_GROUT
    0.73
  BHE_PIPE_DISTANCE
    0.053

#STOP
```

6.2 Simulation Results

The evolution of outlet temperatures and COP of both models is shown for the first ten years in Fig. 6.3. For the model without heat pump, the COP values are computed as a post-processing result based on the BHE outlet temperatures. That means, the dynamic regulation of the BHE load according to Eqs. (3.1) and (3.2) is not included in this model. Therefore, we observe much lower outlet temperatures and COP values, when the heat pump is not considered. This is also reflected in the statistical distribution of the COP for all heating periods, which is shown in Fig. 6.4.

The consumption of electrical energy by the heat pump can be computed by

$$E_{el} = \int \frac{\dot{Q}_{BHE}(t)}{COP(t)} dt. \tag{6.4}$$

With an assumed electricity price of 0.28 Euro kWh^{-1}, the operational costs for the GSHP system evaluate to 29,994 Euro. For the model without heat pump integration, the operational costs evaluate to 43,067 Euro. Please note, that the computation of COP evolution and operational costs for the model without heat pump are carried out here only for demonstration purposes. As can be clearly seen, evaluation of these values leads to completely wrong results, as the COP-corrected dynamic load boundary condition is missing.

As an exemplary results, the soil temperature distribution on a cross-section at the BHE location after 30 years of operation is shown in Fig. 6.5.

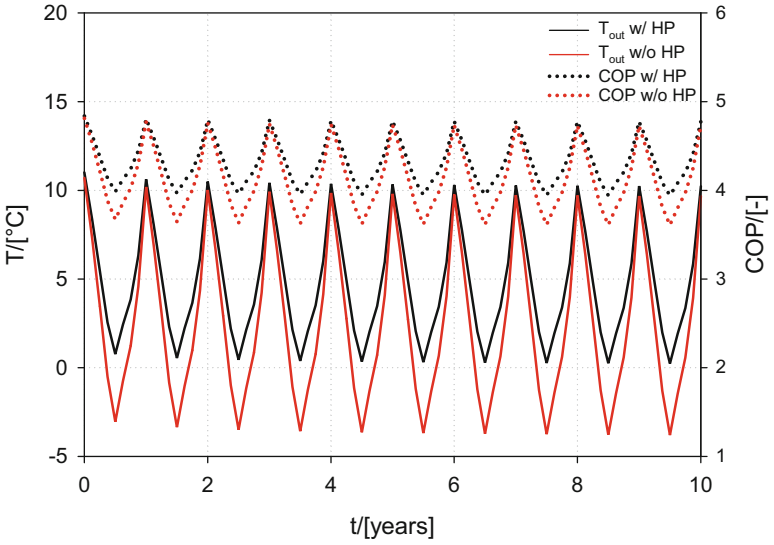

Fig. 6.3 Evolution of BHE outlet temperatures and COP

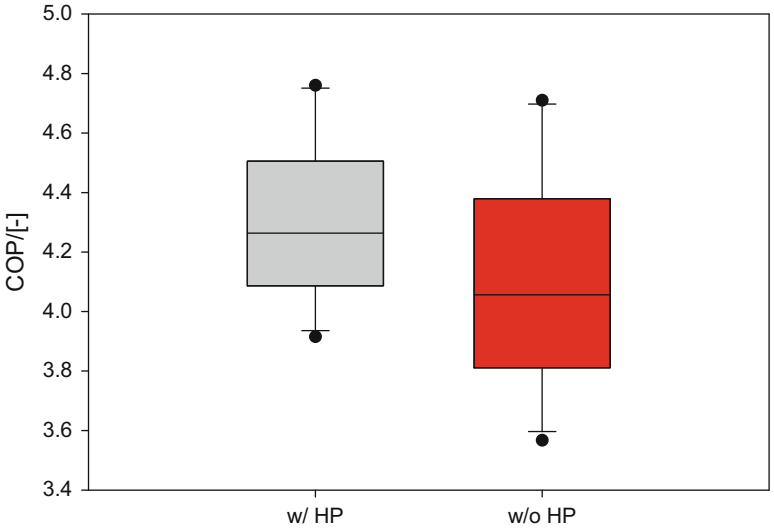

Fig. 6.4 Statistical distribution of COP

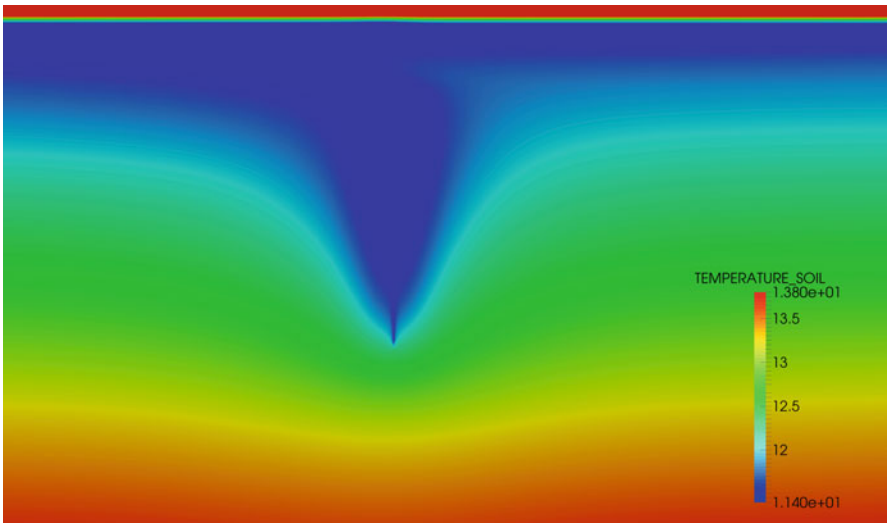

Fig. 6.5 Soil temperature distribution after 30 years of operation

6.3 Implifications of the Model

6.3.1 Overall Dynamics of the BHE Coupled GSHP System

Figure 6.3 shows the dynamics of BHE outflow temperature over a 10 years of time. Within a heating period, the soil surrounding the BHE will first be cooled, this also leads to a cold plume around the BHE (cf. Fig. 6.5). Along with the temperature drop, a steep gradient will form between the BHE and the soil in the vicinity of it. This means, the heat transfer process will be enhanced, and sensible heat in the subsurface will be driven by such gradient and eventually be collected by the BHE. If the BHE keeps extracting heat, the size of the plume will increase, until a quasi steady-state is reached, i.e. the soil temperature distribution only changes very little over time. As illustrated in Fig. 6.3, once the heating period is over, the heat will still be driven by the gradient, to make the soil temperature to recover.

6.3.2 The Role of the Heat Pump

It should be noticed that, for a realistic simulation of the GSHP system, the heat pump dynamics is also an essential part and cannot be ignored. As shown in Fig. 6.3, when the heat pump is involved, the modelled outflow temperature will be consistently higher than the profile without it. This is because, the heat pump acts as a buffer between the building thermal load and the BHE. When a strong thermal load

is imposed on the BHE, the outflow temperature will drop in response. Meanwhile, the heat pump efficiency, in terms of COP value, will also drop correspondingly. This means, more heat will be supplied by the electricity consumption, rather an heat extracted from the subsurface. As a result, the outflow temperature in the reality, where a heat pump is always coupled, will be higher than the simulated scenario, in which the building thermal load is directly imposed on the BHE.

6.3.3 *The Price of Under-Design*

With the above heat pump featured in mind, one may argue that under-design of the BHE system might be beneficial. Since electricity price in many counties is relatively low, and drilling cost is very high. It could be an overall beneficial choice, to save on the initial investment by drilling a shorter BHE, and pay more on the electricity bill over years. By using the Leipzig-area model presented above, a numerical experiment has been conducted. Here, the engineers were assumed to have designed the BHE system based on a soil thermal conductivity value of 2.4 W m^{-1} K^{-1}, while the actual *lambda* values is only 2.1, 1.8, 1.5 and 1.2 W m^{-1} K^{-1}. The corresponding minimum outflow and soil temperature profiles were depicted in Fig. 6.6. It can be observed that, with a lower real *lambda* value, the outflow temperature every year will be considerably lower. One could imagine, that

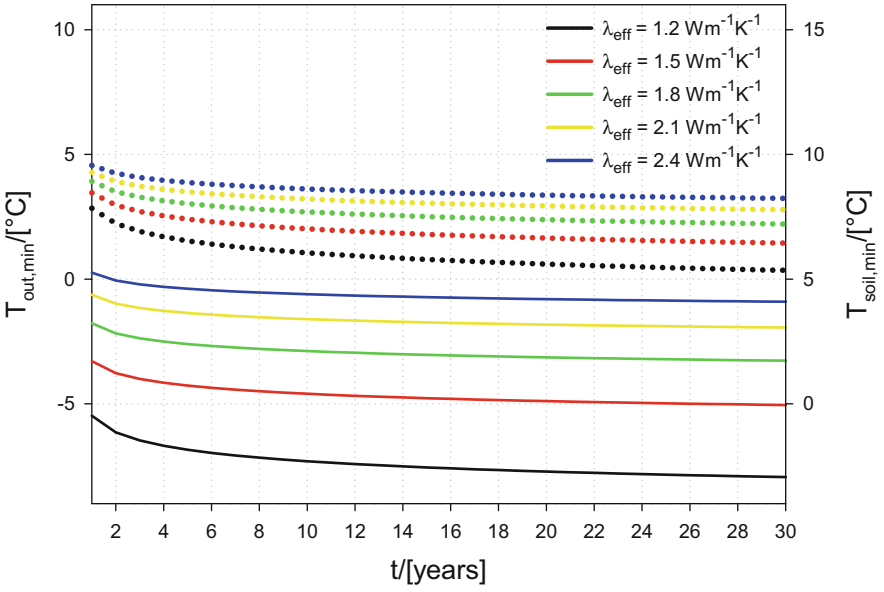

Fig. 6.6 Evolution of minimum soil and outflow temperature, by incorrectly assumed thermal conductivity values of the subsurface (under-design scenarios after Hein et al. 2016)

the heat pump will be running under an unfavourable condition. More importantly, with a severe under-design, the outflow temperature can drop down to as low as −5 °C. For most heat pump systems, such a sharp drop in the outflow temperature will cause a sudden system shut-down during the cold winter. Therefore, a site-specific subsurface investigation will be essential to the long-term success of BHE coupled GSHP system.

Chapter 7
Summary and Outlook

After talking a lot about how to numerically model the heat transport process induced by a GSHP system, a few advices can be given to the end users, which were obtained by the authors through various modelling studies.

- Before designing a GSHP system, it is recommended to obtain the subsurface characteristics as accurately as possible. For example, the identification of aquifer and groundwater can greatly enhance the efficiency of the borehole heat exchangers, leading to a much shorter BHE and lower drilling cost. On the other side, if the thermal conductivity of the soil is over-estimated, a under-designed system can quickly run into trouble after a few years of operation.
- Make sure to conduct proper grouting inside the BHE. This is not only required by the regulation to prevent groundwater contamination. Actually, a poorly grouted BHE with air pocket in it is eventually a BHE with smaller surface area for heat exchange. When possible, a thermally enhanced grout should be applied, as simulation based result suggests that the additional investment will quickly be paid off after couple of years' operation (cf. Hein et al. 2016).
- Try to avoid multiple BHEs located in a close vicinity. The distance between BHEs is recommended to be larger than 10 m. Simulation results has suggested that the thermal plume from adjacent BHEs is very likely to interfere with each other. There are cases where the BHEs are drilled very close to each other and the system performance starts to drop after a few years of operation.

As mentioned above, more and more commercial buildings are now equipped with BHE coupled GSHP systems. In such cases, often dozens or even hundreds of BHEs are connected to each other and drilled in a small piece of land. These big systems can not be simulated yet by the OpenGeoSys software in its current stage. Currently, research has already been started on this front, and readers could expect an updated tutorial focusing on this topic in the near future.

H. Shao et al., *Geoenergy Modeling II*, SpringerBriefs in Energy,
DOI 10.1007/978-3-319-45057-5_7

Appendix A
Symbols

The symbols used in the tutorial is summarized in Table A.1.

Table A.1 Table of Symbols

Symbol	Parameter	Unit
Latin symbols		
$\mathbf{A}$	Global system matrix	
a	Heat transfer coefficient	$\mathrm{W \cdot K^{-1} \cdot m^{-2}}$
$\mathbf{b}$	Right-hand-side vector	
c	Specific heat capacity	$\mathrm{J \cdot kg^{-1} \cdot K^{-1}}$
Cr	Courant number, criteria	
$\mathbf{D}$	Diagonal matrix	
e	Specific energy	$\mathrm{J \cdot kg^{-1}}$
e_k	Iteration error	
$\mathbf{g}$	Gravity acceleration vector	$\mathrm{m \cdot s^{-1}}$
h	Specific enthalpy	$\mathrm{J \cdot kg^{-1}}$
$\mathbf{j}_{\mathrm{adv}}$	Advective heat flux	$\mathrm{W \cdot m^{-2}}$
$\mathbf{j}_{\mathrm{diff}}$	Diffusive heat flux	$\mathrm{W \cdot m^{-2}}$
$\mathbf{j}_{\mathrm{disp}}$	Dispersive heat flux	$\mathrm{W \cdot m^{-2}}$
$\mathbf{J}$	Jacobian	
$\mathbf{k}$	Permeability tensor	$\mathrm{m^2}$
k_{rel}	Relative permeability	–
$\mathbf{K}^{(e)}$	Element conductivity matrix	
$\mathbf{L}$	Differential operator	
$\hat{L}$	Approximation operator	
$\mathbf{L}$	Lower matrix	
$L^{(e)}$	Element length	
m	Mass	kg
n	Porosity	$\mathrm{m^3 \cdot m^{-3}}$
$\mathbf{N}^{(e)}$	Element shape function	
Ne	Neumann number, criteria	

H. Shao et al., *Geoenergy Modeling II*, SpringerBriefs in Energy,
DOI 10.1007/978-3-319-45057-5

Symbol	Parameter	Unit
q^i	Internal heat source	$\mathrm{J\,kg^{-1}\,s^{-1}}$
$\mathbf{q}$	Darcy flux, velocity	$\mathrm{m\,s^{-1}}$
Q	Amount of heat	J
Q_T	Heat production term (volumetric)	$\mathrm{J\,m^{-3}\,s^{-1}}$
q_T	Heat production term (specific)	$\mathrm{kg^{-1}\,s^{-1}}$
$\mathbf{R}$	Residuum vector	
S	Saturation	–
t	Time	s
T	Temperature	K
u	Internal energy	$\mathrm{J\,kg^{-1}}$
$u(t,x)$	Unknown field function of time and space	
u_j^n	Unknown field function approximation at time level n in node j	
$\mathbf{U}$	Upper matrix	
$\mathbf{v}$	Velocity vector	$\mathrm{m\,s^{-1}}$
V	Volume	$\mathrm{m^3}$
$\mathbf{x}$	Solution vector	
Greek symbols		
$\boldsymbol{\alpha}$	Diffusivity	$\mathrm{m^2\,s^{-1}}$
$\boldsymbol{\lambda}$	Thermal conductivity	$\mathrm{W\,K^{-1}\,m^{-1}}$
ρ	Density	$\mathrm{kg\,m^{-3}}$
Δ	Difference	–
ϵ	Volume fraction	–
ϵ_j^n	Approximation error at time level n in node j	–
ψ	Conservation quantity	–
$\boldsymbol{\sigma}$	Stress tensor	Pa
μ	Viscosity	Pa s
Exponents, indices		
i,j	Node numbers	
k	Non-linear iteration number	
n	Time level	
s	Solid	
l	Liquid	
w	Water	
f	Fluid	
α	All phases	
γ	Fluid phases	

Appendix B
Keywords

This section provides a wrap-up compendium of the OGS keywords used in this tutorial. A more comprehensive compilation of OGS keywords you can find at www.opengeosys.org/help/documentation/.

B.1 GLI: Geometry

Listing B.1 GLI keyword

```
#POINTS                // points keyword
0 0 0 0 $NAME POINT0   // point number | x | y | z | point name
1 1 0 0 $NAME POINT1   // point number | x | y | z | point name
#POLYLINE              // polyline keyword
 $NAME                 // polyline name subkeyword
  LINE                 // polyline name
 $POINTS               // polyline points subkeyword
  0                    // point of polyline
  1                    // dito
#STOP                  // end of input data
```

OGS Weblink:
http://www.opengeosys.org/help/documentation/geometry-file

B.2 MSH: Finite Element Mesh

Listing B.2 MSH keyword

```
#FEM_MSH      // file/object keyword
$NODES        // node subkeyword
61            // number of grid nodes
0 0 0 0       // node number x y z
```


H. Shao et al., *Geoenergy Modeling II*, SpringerBriefs in Energy,
DOI 10.1007/978-3-319-45057-5

```
1 0 0 1       // dito
...
59      0       0       59
60      0       0       60
$ELEMENTS      // element subkeyword
60             // number of elements
0       0       line    0       1  // element number | material group number |
     element type | element node numbers
1       0       line    1       2  // dito
...
58      0       line    58      59 // dito
59      0       line    59      60 // dito
#STOP              // end of input data
```

OGS Weblink:
http://www.opengeosys.org/help/documentation/mesh-file

B.3 PCS: Process Definition

Listing B.3 PCS keyword

```
#PROCESS              // process keyword
  $PCS_TYPE           // process type subkeyword
    HEAT_TRANSPORT    // specified process(es)
    GROUNDWATER_FLOW  // dito
    LIQUID_FLOW       // dito
                ...
#STOP                 // end of input data
```

OGS Weblink:
www.opengeosys.org/help/documentation/process-file

B.4 NUM: Numerical Properties

Listing B.4 NUM keyword

```
#NUMERICS         // process keyword
  $PCS_TYPE       // process type subkeyword, see PCS above
  $LINEAR_SOLVER  // linear solver type subkeyword, see table below
         Parameters     // 7 parameters, see table below
#STOP             // end of input data
```

Numerical properties

- Linear solver type (its C++ ;-) numbering −1)
  1. SpGAUSS, direct solver
  2. SpBICGSTAB

3. SpBICG
4. SpQMRCGSTAB
5. SpCG
6. SpCGNR
7. CGS
8. SpRichard
9. SpJOR
10. SpSOR

- Convergence criterion (its C++ ;-) numbering −1)

1. Absolutely error $||r|| < \epsilon$
2. $||r|| < \epsilon||b||$
3. $||rn|| < \epsilon||rn - 1||$
4. if $||rn|| < 1$ then $||rn|| < \epsilon||rn - 1||$ else $||r|| < \epsilon$
5. $||rn|| < \epsilon||x||$
6. $||rn|| < \epsilon \max ||rn - 1||, ||x||, ||b||$

- Error tolerance ϵ, according to the convergence criterion model above
- Maximal number of linear solver iterations
- Relaxation parameter $\theta \in [0, 1]$
- Preconditioner

0 No preconditioner,
1 Jacobi preconditioner,
100 ILU preconditioner.

- Storage model

2 unsymmetrical matrix,
4 symmetrical matrix.

OGS Weblink:
http://www.opengeosys.org/help/documentation/numeric-file

B.5 TIM: Time Discretization

Listing B.5 TIM keyword

```
#TIME_STEPPING     // time stepping keyword
  $PCS_TYPE        // process subkeyword
    HEAT_TRANSPORT // specified process
  $TIME_STEPS      // time steps subkeyword
   1000 390625e+0  // number of times steps | times step length
  $TIME_END        // end time subkeyword
    1E99           // end time value
  $TIME_START      // starting time subkeyword
```

```
    0.0             // starting time value
 $TIME_UNIT         // specified time unit
    DAY             // SECOND, DAY, YEAR
#STOP               // end of input data
```

OGS Weblink:
http://www.opengeosys.org/help/documentation/time-step-control-file

B.6 IC: Initial Conditions

Listing B.6 IC keyword

```
#INITIAL_CONDITION  // initial conditions keyword
 $PCS_TYPE          // process subkeyword
  HEAT_TRANSPORT    // specified process
 $PRIMARY_VARIABLE  // primary variable subkeyword
  TEMPERATURE1      // specified primary variable
 $GEO_TYPE          // geometry subkeyword
  DOMAIN            // specified geometry: entire domain (all nodes)
 $DIS_TYPE          // distribution subkeyword
  CONSTANT   0      // specified distribution: constant value 0 at DOMAIN
     geometry
#STOP               // end of input data
```

OGS Weblink:
http://www.opengeosys.org/help/documentation/initial-condition-file

B.7 BC: Boundary Conditions

Listing B.7 BC keyword

```
#BOUNDARY_CONDITION // boundary condition keyword
 $PCS_TYPE          // process type subkeyword
  HEAT_TRANSPORT    // specified process
 $PRIMARY_VARIABLE  // primary variable subkeyword
  TEMPERATURE1      // specified primary variable
 $GEO_TYPE          // geometry type subkeyword
  POINT POINT0      // specified geometry type | geometry name
 $DIS_TYPE          // boundary condition type subkeyword
  CONSTANT   1      // boundary condition type | value
#STOP               // end of input data
```

OGS Weblink:
http://www.opengeosys.org/help/documentation/boundary-condition-file

B.8 ST: Source/Sink Terms

Listing B.8 ST keyword

```
#SOURCE_TERM             // source term keyword
 $PCS_TYPE               // process type subkeyword
  LIQUID_FLOW            // specified process
 $PRIMARY_VARIABLE       // primary variable subkeyword
  PRESSURE1              // specified primary variable
 $GEO_TYPE               // geometry type subkeyword
  POINT POINT0           // specified geometry type | geometry name
 $DIS_TYPE               // boundary condition type subkeyword
  CONSTANT_NEUMANN 1E-6  // source term type | value
#STOP                    // end of input data
```

OGS Weblink:
http://www.opengeosys.org/help/documentation/source-term-file

B.9 MFP: Fluid Properties

Listing B.9 MFP keyword

```
#FLUID_PROPERTIES         // fluid properties keyword
 $DENSITY                 // fluid density subkeyword
  4 1000 0 -0.2           // type (4: temperature dependent) | 2 values
 $VISCOSITY               // fluid viscosity subkeyword
  1 0.001                 // type (1: constant value) | value
 $SPECIFIC_HEAT_CAPACITY // specific heat capacity subkeyword
  1 4200.0                // type (1: constant value) | value
 $HEAT_CONDUCTIVITY       // thermal heat conductivity subkeyword
  1 0.65                  // type (1: constant value) | value
#STOP                     // end of input data
```

OGS Weblink:
http://www.opengeosys.org/help/documentation/fluid-properties-file
See Table B.1.

Table B.1 Density models

Model	Meaning	Formula	Parameters
0	Curve	RFD file	
1	Constant value	ρ_0	Value of ρ_0
2	Pressure dependent	$\rho(p) = \rho_0(1 + \beta_p(p - p_0))$	ρ_0, β_p, p_0
3	Salinity dependent	$\rho(C) = \rho_0(1 + \beta_C(C - C_0))$	ρ_0, β_p, C_0
4	Temperature dependent	$\rho(p) = \rho_0(1 + \beta_T(T - T_0))$	ρ_0, β_T, T_0
...	...	...	...

B.10 MSP: Solid Properties

Listing B.10 MSP keyword

```
#SOLID_PROPERTIES // solid properties keyword
  $DENSITY        // solid density subkeyword
    1 2500        // type (1: constant value) | value
  $THERMAL        // thermal properties subkeyword
    EXPANSION:    // thermal expansion
    1.0e-5        // values
  CAPACITY:       // heat capacity
    1 1000        // type (1: constant value) | value
  CONDUCTIVITY:   // thermal conductivity
    1 3.2         // type (1: constant value) | value
#STOP             // end of input data
```

OGS Weblink:
TBD

B.11 MMP: Porous Medium Properties

Listing B.11 MMP keyword

```
#MEDIUM_PROPERTIES      // solid properties keyword
 $GEOMETRY_DIMENSION    // dimension subkeyword
  1                     // 1: one-dimensional problem
 $GEOMETRY_AREA         // geometry area subkeyword
  1.0                   // value in square meter if 1D
 $POROSITY              // porosity subkeyword
  1  0.10               // type (1: constant value) | value
 $STORAGE               // storativity subkeyword
  1  0.0                // type (1: constant value) | value
 $TORTUOSITY            // tortuosity subkeyword
  1  1.000000e+000      // type (1: constant value) | value
 $PERMEABILITY_TENSOR   // permeability subkeyword
  ISOTROPIC   1.0e-15   // tensor type (ISOTROPIC) | value(s)
 $HEAT_DISPERSION       // porosity subkeyword
  1  0.0e+00 0.0e+00    // type (1: constant values) | longitudinal |
    transverse
                             // thermal dispersion length
#STOP                   // end of input data
```

OGS Weblink:
http://www.opengeosys.org/help/documentation/material-properties-file

B.12 OUT: Output Parameters

Listing B.12 OUT keyword

```
#OUTPUT           // output keyword
 $PCS_TYPE        // process subkeyword
  HEAT_TRANSPORT // specified process
 $NOD_VALUES      // nodal values subkeyword
  TEMPERATURE1    // specified nodal values
 $GEO_TYPE        // geometry type subkeyword
  POLYLINE ROCK   // geometry type and name
 $TIM_TYPE        // output times subkeyword
  STEPS 1         // output methods and parameter
#STOP             // end of input data
```

OGS Weblink:
http://www.opengeosys.org/help/documentation/output-control-file

References

Al-Khoury, R., Kölbel, T., Schramedei, R.: Efficient numerical modeling of borehole heat exchangers. Comput. Geosci. **36**(10), 1301–1315 (2010). ISSN 0098-3004. doi:http://dx.doi.org/10.1016/j.cageo.2009.12.010

Arola, T., Korkka-Niemi, K.: The effect of urban heat islands on geothermal potential: examples from quaternary aquifers in finland. Hydrogeol. J. **22**(8), 1953–1967 (2014). ISSN 1435-0157. doi:10.1007/s10040-014-1174-5

Bauer, S., Beyer, C., Dethlefsen, F., Dietrich, P., Duttmann, R., Ebert, M., Feeser, V., Görke, U., Köber, R., Kolditz, O., Rabbel, W., Schanz, T., Schäfer, D., Würdemann, H., Dahmke, A.: Impacts of the use of the geological subsurface for energy storage: an investigation concept. Environ. Earth Sci. **70**(8), 3935–3943 (2013)

Beier, R.A., Smith, M.D., Spitler, J.D.: Reference data sets for vertical borehole ground heat exchanger models and thermal response test analysis. Geothermics **40**(1), 79–85 (2011). doi:10.1016/j.geothermics.2010.12.007

Cacace, M., Blöcher, G., Watanabe, N., Moeck, I., Börsing, N., Scheck-Wenderoth, M., Kolditz, O., Huenges, E.: Modelling of fractured carbonate reservoirs: outline of a novel technique via a case study from the molasse basin, southern bavaria, germany. Environ. Earth Sci. **70**(8), 3585–3602 (2013)

Casasso, A., Sethi, R.: Efficiency of closed loop geothermal heat pumps: a sensitivity analysis. Renew. Energy **62**, 737–746 (2014)

Clauser, C.: Thermal Signatures of Heat Transfer Processes in the Earth's Crust. Springer, Heidelberg (1999). ISBN 3-540-65604-9

Diersch, H.-J.G., Bauer, D., Heidemann, W., Rühaak, W., Schätzl, P.: Finite element modeling of borehole heat exchanger systems: part 1. Fundamentals. Comput. Geosci. **37**(8), 1122–1135 (2011a). ISSN 0098-3004. doi:http://dx.doi.org/10.1016/j.cageo.2010.08.003

Diersch, H.-J.G., Bauer, D., Heidemann, W., Rühaak, W., Schätzl, P.: Finite element modeling of borehole heat exchanger systems: part 2. Numerical simulation. Comput. Geosci. **37**(8), 1136–1147 (2011b). ISSN 0098-3004. doi:http://dx.doi.org/10.1016/j.cageo.2010.08.003

Diersch, H.-J.: FEFLOW Finite Element Modeling of Flow, Mass and Heat Transport in Porous and Fractured Media. Springer, Heidelberg (2014)

Eicker, U., Vorschulze, C.: Potential of geothermal heat exchangers for office building climatisation. Renew. Energy **34**(4), 1126–1133 (2009).

Glen Dimplex Deutschland GmbH: Heat pump SI30TER+, equipment data (2016). http://www.dimplex.de/pdf/de/produktattribute/produkt_1722822_extern_egd.pdf

H. Shao et al., *Geoenergy Modeling II*, SpringerBriefs in Energy,
DOI 10.1007/978-3-319-45057-5

Hein, P., Kolditz, O., Görke, U.-J., Bucher, A., Shao, H.: A numerical study on the sustainability and efficiency of borehole heat exchanger coupled ground source heat pump systems. Appl. Therm. Eng. **100**, 421–433 (2016). ISSN 1359–4311. doi:http://dx.doi.org/10.1016/j.applthermaleng.2016.02.039

Huenges, E., Kohl, T., Kolditz, O., Bremer, J., Scheck-Wenderoth, M., Vienken, T.: Geothermal energy systems: research perspective for domestic energy provision. Environ. Earth Sci. **70**(8), 3927–3933 (2013)

Jaszczur, M., Śliwa, T.: The analysis of long-term borehole heat exchanger system exploitation. Comput. Assist. Methods Eng. Sci. **20**(3), 227–235 (2013)

Kahraman, A., Çelebi, A.: Investigation of the performance of a heat pump using waste water as a heat source. Energies **2**(3), 697–713 (2009)

Kolditz, O., Jakobs, L.A., Huenges, E., Kohl, T.: Geothermal energy: a glimpse at the state of the field and an introduction to the journal. Geotherm. Energy **1** (2013). doi:10.1186/2195-9706-1-1

Leipzig Institute for Meteorology - LIM, Faculty of Physics and Earth Sciences, University Leipzig: Weather and climate archive data (Wetter & Klima, Archivdaten) (2016). http://www.uni-leipzig.de/~meteo/en/wetterdaten/archiv.php

Panteleit, B., Reichling, J.: Automatical assignement of petrographic parameters for optimized ground-source heat pumps (Automatisierte Attribuierung von Bohrungsdaten mit Parametern zur Optimierung von Erdwärmesondenanlagen). Grundwasser **11**(1), 19–26 (2006). doi:10.1007/s00767-006-0115-1

Richter, M., Huber, C., Reinhardt, K., Wachmann, H., Gerschel, A.: Potential of heat supply for Saxon gardening companies utilizing geothermal energy as subject to site-specific geological conditions and different business organisations/utilisation concepts (Möglichkeiten der Wärmeversorgung von sächsischen Gartenbaubetrieben mit Geothermie in Abhängigkeit von geologischen Standortfaktoren und verschiedenen Betriebsstrukturen/Nutzungskonzepten) (2015)

Sanner, B., Karytsas, C., Mendrinos, D., Rybach, L.: Current status of ground source heat pumps and underground thermal energy storage in europe. Geothermics **32**(4), 579–588 (2003)

Scheck-Wenderoth, M., Schmeisser, D., Mutti, M., Kolditz, O., Huenges, E., Schultz, H.-M., Liebscher, A., Bock, M.: Geoenergy: new concepts for utilization of geo-reservoirs as potential energy sources. Environ. Earth Sci. **70**(8), 3427–3431 (2013)

Speer, S.: Design calculations for optimising of a deep borehole heat-exchanger. Master's thesis, RWTH Aachen University, Aachen (2005)

Stauffer, F., Bayer, P., Blum, P., Molina-Giraldo, N., Kinzelbach, W.: Thermal Use of Shallow Groundwater. Taylor & Francis Group, Boca Raton (2014)

The Association of German Engineers (Verein Deutscher Ingenieure): VDI guideline 4640: thermal use of the underground – part 2: ground source heat pump systems, draft (VDI Richtlinie 4640: Thermische Nutzung des Untergrunds - Blatt 2: Erdgekoppelte Wärmepumpenanlagen, Entwurf) (2015)

Zheng, T., Shao, H., Schelenz, S., Hein, P., Vienken, T., Pang, Z., Kolditz, O., Nagel, T.: Efficiency and economic analysis of utilizing latent heat from groundwater freezing in the context of borehole heat exchanger coupled ground source heat pump systems. Appl. Therm. Eng. **105**, 314–326 (2016). ISSN 1359–4311. doi:http://dx.doi.org/10.1016/j.applthermaleng.2016.05.158

Zhu, K., Blum, P., Ferguson, G., Balke, K.-D., Bayer, P.: The geothermal potential of urban heat islands. Environ. Res. Lett. **5**(4), 044002 (2010)